Dicarboxylic acids, ω-oxocarboxylic acids, α-dicarbonyls, WSOC, OC, EC, and inorganic ions in wintertime size-segregated aerosols from central India: sources and formation processes

Dhananjay K. Deshmukh[1,a,*], Kimitaka Kawamura[1,a,*] and Manas K. Deb[2]

[1]Institute of Low Temperature Science, Hokkaido University, Sapporo 060-0819, Japan

[2]School of Studies in Chemistry, Pt. Ravishankar Shukla University, Raipur 492010, India

[a]Now at Chubu Institute for Advanced Studies, Chubu University, Kasugai 487-8501, Japan

*Correspondence to: D.K. Deshmukh (deshmukh@pop.lowtem.hokudai.ac.jp) and K. Kawamura (kkawamura@isc.chubu.ac.jp)

Abstract

The size distributions of aerosols can provide evidences for their sources and formation processes in the atmosphere. Size-segregated aerosols (9-sizes) were collected in urban site (Raipur: 21.2°N and 82.3°E) in central India during winter of 2012-2013. The samples were analyzed for dicarboxylic acids (C_2-C_{12}), ω-oxocarboxylic acids (ωC_2-ωC_9), pyruvic acid and α-dicarbonyls (C_2-C_3) as well as elemental carbon (EC), organic carbon (OC), water-soluble OC (WSOC) and inorganic ions. Diacids showed a predominance of oxalic acid (C_2) followed by succinic and azelaic acid whereas ω-oxoacids exhibited a predominance of glyoxylic acid and glyoxal was more abundant than methylglyoxal in all the sizes. Diacids, ω-oxoacids and α-dicarbonyls showed bimodal size distribution with peaks in fine and coarse modes. High correlations of fine mode diacids and related compounds with potassium and levoglucosan suggest that they were presumably due to a substantial contribution of primary emission from biomass burning and secondary production from biomass burning derived precursors. High correlations of C_2 with higher carbon number diacids (C_3-C_9) suggest that they have similar sources and C_2 may be produced via the decay of its higher homologues diacids in fine mode. Considerable portions of diacids and related compounds in coarse mode suggest that they were associated with mineral dust particles by their adsorption and photooxidation of anthropogenic and biogenic precursors via heterogeneous reaction on dust surface. This study demonstrates that biomass burning and dust particles are two major factors to control the size distribution of diacids and related compounds in the urban aerosols from central India.

Keywords: Water-soluble dicarboxylic acids; inorganic species; size distributions; biomass burning; dust particles; primary and secondary sources.

1. Introduction

Aerosols influence the global climate directly by scattering or absorbing solar radiation and indirectly by altering cloud microphysics and hydrological cycle (Ramanathan et al., 2007). The direct and indirect effects are associated with the physical and chemical properties of atmospheric particles. The knowledge of size distributions of aerosols and their chemical composition is needed to understand their effect on climate change (Kanakidou et al., 2005), source identification (Davidson et al., 2005; Pant et al., 2016), and human health (Tremblay et al., 2007). Homologous series of water-soluble dicarboxylic acids and related compounds are identified in aerosols from many regions of the world including the urban (Kawamura and Yasui, 2005; Ho et al., 2006; Miyazaki et al., 2009; Agarwal et al., 2010; Wang et al., 2012; Van Pinxteren et al., 2014), marine (Kawamura and Sakaguchi, 1999; Mochida et al., 2007; Fu et al., 2013; Zhang et al., 2016a), and polar atmosphere (Kawamura et al., 1996a; Kawamura et al., 1996b; Kerminen et al., 1999). They play a crucial role in the hygroscopic growth of aerosols and the activation of cloud condensation nuclei (CCN) (Turpin et al., 2000; Prenni et al., 2003).

The primary sources of diacids and related compounds are fossil fuel combustion and biomass burning (Chebbi and Carlier, 1996; Kundu et al., 2010a; Mkoma and Kawamura, 2013). The photooxidation of unsaturated fatty acids (UFAs) and volatile organic compounds (VOCs) of biogenic and anthropogenic origin are their secondary sources (Kawamura et al., 1996a; Huang et al., 2005; Tsai and Kuo, 2013). Oxalic acid (C_2) is usually the most abundant diacid in atmospheric aerosols with concentration ranging from a few ng m^{-3} in remote locations (Kawamura et al., 1996a) to hundreds or even up to one thousand ng m^{-3} in urban regions (Ho et al., 2007). Laboratory studies and field measurements suggest that C_2 is mostly produced via aqueous-phase oxidation of glyoxal (Gly), methylglyoxal (MeGly), and longer-chain diacids (C_3-C_{12}), which are oxidation intermediates of various VOCs and UFAs (Ervens et al., 2004; Carlton et al., 2007; Lim et al., 2005; Enami et al., 2015; Pavuluri et al., 2015; Kawamura and Bikkina, 2016; Zhang et al., 2016a).

South Asia is one of the most important source regions for aerosols on the globe because of the huge emissions from anthropogenic activities, contributing significantly to global climate change (Ramanathan et al., 2007; Gustafsson et al., 2009). The emission of aerosols is potentially large in this region due to the rising economies in India and extensive use of biofuels and biomass that contributes 85-90% of cooking energy (Chowdhuri et al., 2007). Dumping of solid wastes from urban areas into open landfills and regular burning without any emission control is also a potential source of aerosols in India (Pavuluri et al., 2010; Kawamura and Pavuluri, 2010). The atmosphere of Raipur in winter is highly affected from biofuel and biomass burning emission (Verma et al., 2010; Deshmukh et al., 2013). Coal and wood combustion is usually used for energy sources in this region. A National Highway known as Great Eastern Road with high vehicular traffics adds to the emission of particulate pollutants in this region. There are other major sources of aerosols in the surrounding of Raipur, including an industrial hub, residential burning, burning of agricultural crop residues in the open fields, and resuspended soil dust.

The transport of anthropogenic and biomass burning derived aerosols from the Indo-Gangetic Plain (IGP) also significantly influences the air quality of Raipur. Nirmalkar et al. (2015) reported that biomass burning and fossil fuel combustion are the dominant emission sources for high levels of organic compounds in eastern central India. With this background Raipur is a unique place to investigate the atmospheric chemistry and processes of diacids and related compounds. A few studies on diacids and related compounds in India have been made in bulk aerosols (Miyazaki et al., 2009; Pavuluri et al., 2010; Hegde and Kawamura, 2012). There is no study on the size distributions of diacids and related compounds in the atmosphere of India.

Nine-size fractions of winter aerosols were collected in the urban atmosphere of Raipur in central India. The samples were analyzed for homologous series of diacids (C_2-C_{12}), ω-oxoacids (ωC_2-ωC_9) and α-dicarbonyls (C_2-C_3) on a molecular level. Organic carbon (OC) and elemental carbon (EC) as well as water-soluble OC (WSOC) and inorganic ions were also analyzed. The goals of this study were to investigate the size distribution of diacids and related compounds and evaluate

their sources and formation processes. The potential factors responsible for their size distributions and the atmospheric implications of the size characteristics are discussed.

2. Materials and method

2.1. Site description and aerosol collection

The collection of size-segregated samples was performed in the city of Raipur (21.2°N and 82.3°E, elevation of 297 m above the sea level) in central India. The location of sampling site and its surroundings are shown in Fig. 1. Total area of the city is 226 km^2. Raipur has population of 1.2 million as per the Census of India 2011 (Deshmukh et al., 2013). The use of biomass such as wood-fuel and crop residues for cooking and heating purpose in Raipur releases a huge amount of organic compounds to the atmosphere in central India (Deshmukh et al., 2013). Burning of agricultural residues in the open field is common after crop harvesting in central India, which usually begins in December and continues till the end of January. A significant amount of organic compounds is also released from different kinds of industrial operation and motor vehicles. Open burning of domestic and municipal solid waste and re-suspension of dust particles are another important sources of atmospheric particles over central India. Raipur is also a receptor site of transported aerosols from the IGP areas, which are enriched with burning products of crop residues and industrial emissions.

Size-segregated samples (n = 13) were collected in winter of 2012-2013 on a rooftop of chemical science building about 15 m above the ground level at Ravishankar Shukla University campus using an Andersen sampler model TE 20-800 (USA) with a flow rate of 28.3 L min^{-1}. Each set of sample comprises of nine filters with various sizes of D_p < 0.43, 0.43-0.65, 0.65-1.1, 1.1-2.1, 2.1-3.3, 3.3-4.7, 4.7-5.8, 5.8-9.0, and > 9.0 µm. The sampler was equipped with 80 mm quartz fiber filters that were pre-baked at 500°C for 6 hrs. The sample collection time was 96 hrs to obtain enough materials for the chemical analysis. The filters were placed in a pre-baked clean glass vials with a Teflon-lined screw cap and kept frozen in darkness at -20°C to avoid the microbial loss of organic compounds. One set of field blank was collected during the study period.

2.2. Chemical analysis

2.2.1. Dicarboxylic acids and related compounds

The samples were analyzed for water-soluble diacids (C_2-C_{12}), ω-oxoacids (ωC_2-ωC_9) and α-dicarbonyls (C_2-C_3) using a capillary gas chromatography (GC) equipped with a flame ionization detector (FID) (Kawamura and Ikushima, 1993; Kawamura, 1993). A part of the sample filter was extracted with organic-free ultrapure water (>18.2 MΩ cm^{-1}) under ultrasonication. The water extracts were passed through a glass column packed with quartz wool to remove filter debris and insoluble particles. The pH of the extracts was adjusted to 8.5-9.0 using 0.05 M KOH solution prior to dryness to convert carboxylic acids into salt forms for improving the recovery of smaller diacids (Hegde and Kawamura, 2012; Wang et al., 2012). The extracts were concentrated to dryness using a rotary evaporator under vacuum and derivatized with 14% BF_3 in *n*-butanol at 100°C. Acetonitrile and *n*-hexane was added into the derivatized sample and washed with organic-free ultrapure water. The hexane layer containing butyl esters was concentrated and dried by N_2 blow-down and dissolved in a known volume of *n*-hexane.

A 2 μL aliquot of the sample was injected into a Hewlett-Packard HP6890 series GC equipped with a fused silica capillary column and FID detector. Peak identification was performed by comparison of the GC retention times with those of authentic standards. Identification of detected compounds was confirmed by mass spectral examination using a GC-mass spectrometer. Recoveries of diacids performed by spiking authentic standards to a pre-baked quartz fiber filter were 86-90% for C_2 diacid and more than 92% for C_3-C_6 diacids. The precision in the triplicate analysis of the filter sample was 10% for major diacids and related compounds.

2.2.2. Levoglucosan

Levoglucosan was determined using a Dionex ICS-2500 ion chromatography (IC) equipped with a pulsed amperometric detector (PAD), GP50 gradient pump coupled to a Teflon injection valve with 400 μL sample loop, CarboPac MA1 guard column and anion-exchange analytical column. Dionex ED50 electrochemical detector was used with a gold working electrode and pH electrode as reference. 200-600 mM gradient with NaOH was used as an eluent at a flow rate of 0.4 mL min^{-1}.

Dissolution of carbonate into NaOH may result in poor separation during elution and hence care was taken to avoid exposure to atmospheric CO_2.

2.2.3. Water-soluble organic carbon (WSOC)

A punch of 20 mm of each filter was extracted with organic-free ultrapure water in a 50 mL glass vial under ultrasonication for 15 min. The extracts were passed through a syringe filter (Millex-GV, Millipore) of pore size 0.22 µm. The extract was acidified with 1.2 M HCl and purged with pure air to remove dissolve inorganic carbon and volatile organics and then WSOC was measured using a Shimadzu total carbon analyzer (TOC-V_{CSH}) (Miyazaki et al., 2011). External calibration was performed using potassium hydrogen phthalate. Each sample was measured three times and the average value was used for the calculation of concentration of WSOC. The analytical error in the triplicate analysis of the filter sample was 5%.

2.2.4. Organic carbon (OC) and elemental carbon (EC)

OC and EC was determined using a Sunset Lab carbon analyzer following the Interagency Monitoring of Protected Visual Environments (IMPROVE) thermal evolution protocol as described in Wang et al. (2005). A filter disc of 1.5 cm^2 was placed in a quartz tube inside the thermal desorption chamber of the analyzer and stepwise heating was applied. Helium (He) gas was used in the first ramp and switched to mixture of He/O_2 in the second ramp. The evolved CO_2 during the oxidation at each temperature step was measured with non-dispersive infrared detector. The analytical error in the triplicate analysis of the filter sample was 5% for OC and EC.

2.2.5. Water-soluble inorganic ions and methanesulfonic acid

A punch of 20 mm of each filter was extracted with organic-free ultrapure water in an ultrasonic bath and filtered through a disc filter of pore size 0.22 µm. The resulting solutions were injected to a Dionex-4500i ion chromatography for the analysis of MSA^-, Cl^-, SO_4^{2-}, NO_3^-, Na^+, NH_4^+, K^+, Ca^{2+} and Mg^{2+} (Verma et al., 2010). The anions were measured by AS12 analytical column and AG12 guard column with ASRS-Ultra Auto-suppressor. The separation of cations was performed using CS12 analytical column and CG12 guard column with CSRS-Ultra Auto-suppressor. The elution

was performed with 2.7 mM Na_2CO_3/0.3 mM $NaHCO_3$ for anions and 20 mM methanesulfonic acid for cations with a flow rate of 1.0 mL min^{-1}. A conductivity detector was used for the detection of ions. The precision in the triplicate analysis of the filter sample was estimated to be 5%.

Field and laboratory blank samples were extracted and analyzed like the real samples. The blank levels of organic and inorganic components were generally 0.1-5% of concentrations of real samples. Concentrations of all the organic and inorganic species reported here were corrected for the blanks.

2.3. Meteorology and air mass back trajectory analysis

Raipur has a tropical wet and dry climate. Daily meteorological data for the sampling period was obtained from the local meteorological station. The ambient air temperature varied from 5.7 to 32.6°C with an average of 20.9±2.7°C during the sampling period. The relative humidity ranged from 23 to 98% with an average of 65±6.1%. The total precipitation was found to be 30.1 mm. The wind speed varied from 1.9 to 8.5 km h^{-1} with an average of 3.8±1.3 km h^{-1}. Prevailing wind direction was northeast and north during the study period.

The air mass backward trajectory was computed using the Hybrid Single-Particle Legrangian Integrated Trajectory (HYSPLIT) model 4.0 developed by the National Oceanic and Atmospheric Administration (NOAA) Air Resources Laboratory (Draxler and Rolph, 2013). The seven-day air mass back trajectory at the arrival height of 500 m above ground level for the observation site during the study period is shown in Fig. 2.

3. Results and discussion

3.1. Chemical characteristics of size-segregated aerosols

The average chemical composition of size-segregated aerosols is shown in Fig. 3. Fine and coarse mode concentrations of inorganic ions and carbonaceous species are given in Table 1. Sulfate dominated the anionic mass followed by nitrate in all the sizes. Ammonium and potassium contributed to a large fraction of cationic mass in fine mode whereas calcium dominated in coarse mode. High abundances of SO_4^{2-} and NO_3^- in size-segregated aerosols suggest a significant

contribution from anthropogenic sources. The enhanced mass abundances of NH_4^+ and K^+ in fine size fractions indicate a significant contribution from biofuel and biomass burning. Fine mode K^+ has been considered a key tracer for biomass burning (Yamasoe et al., 2000; Falkovich et al., 2005). Levoglucosan (1, 6-anhydro-b-D-glucopyranose) is considered as an excellent molecular marker for biomass burning (Simoneit et al., 1999). It is formed by the pyrolysis of cellulose, the main building material of wood and agricultural crop residues, at temperatures higher than 300 °C (Wang et al., 2009). Strong correlations of fine mode K^+ and NH_4^+ with levoglucosan (r = 0.90 and 0.85) further suggest biomass burning as an important source of Raipur aerosols. Back trajectories at the observation site indicate local sources and long-range transport of air masses from the IGP areas. Air masses from the IGP could deliver anthropogenic and biomass burning aerosols to the Raipur region during the campaign. The growing economy and population over the IGP result in a wide range of biomass burning activities such as wood-fuel and agricultural waste burning (Niranjan et al., 2006). High abundances of Ca^{2+} in coarse size fractions suggest a significant contribution of mineral dusts.

3.2. Molecular distributions of dicarboxylic acids and related compounds

Diacids and related compounds measured in Raipur aerosols are given in Table 1 together with their concentrations in the fine and coarse modes. Their molecular distributions in 9-size fractions of aerosols are given in Fig. 4. Oxalic acid (C_2) was found as the most abundant diacid species followed by succinic acid in all the sizes. The predominance of C_2 in size-segregated aerosols is reasonable because C_2 is significantly produced by the gaseous and aqueous oxidation of various VOCs and UFAs of anthropogenic and biogenic origin (Kawamura and Sakaguchi, 1999; Huang et al., 2005; Tedetti et al., 2007), and primarily generated from fossil fuel combustion and biomass burning (Chebbi and Carlier, 1996; Kundu et al., 2010a; Kawamura et al., 2013; Cong et al., 2015).

Azelaic acid (C_9) was found as the third most abundant diacid in all the sizes followed by terephthalic acid (tPh) in fine size bins and phthalic acid (Ph) in coarse size bins. High abundance of C_9 shows its unique source in Raipur aerosols. C_9 is a specific oxidation product of UFAs such as

oleic acid ($C_{18:1}$) (Kawamura and Gagosian, 1987; Huang et al., 2005; Tedetti et al., 2007), which has been abundantly detected in terrestrial higher plant leaves (Agarwal et al., 2010; Wang et al., 2012). C_9 can also be produced by the biomass burning because biomass contains UFAs (Kawamura et al., 2013). It is noted that Hays et al. (2005) found high concentration of oleic acid in the smoke particles from rice straw burning. High abundance of C_9 in this study indicates an enhanced emission of its precursors from biomass burning and terrestrial plants followed by successive photooxidation to C_9 in the atmosphere of central India.

Burning of solid wastes containing plastics may be the source for the high abundance of tPh in Raipur aerosols because tPh is a major species of polyester fibers and plastic bags and bottles (Fu et al., 2010; Kawamura and Pavuluri, 2010). Ph primarily originates from anthropogenic sources such as coal combustion and secondarily produced from the photooxidation of naphthalene (NAP) and other polynuclear aromatic hydrocarbons originated from incomplete combustion of fossil fuels (Kawamura and Kaplan, 1985). High abundance of Ph in size-segregated aerosols indicates a significant contribution of anthropogenic sources such as coal burning in Raipur during the campaign. Raipur has a cluster of coal-based thermal power plant and is known as part of coal belt of India.

ω-Oxoacids (ωC_2-ωC_9), pyruvic acid and α-dicarbonyls (C_2-C_3) are primarily originated from combustion sources and secondarily produced via atmospheric photooxidation of various organic precursors originated from anthropogenic and biogenic sources (Kawamura et al., 1996a; Kawamura and Bikkina, 2016). Glyoxylic acid (ωC_2) was found as the most abundant ω-oxoacid whereas glyoxal (Gly) was found more abundant than methylglyoxal (MeGly) in all the sizes. ωC_2 is initially produced by oxidation of Gly and MeGly in aqueous-phase whereas Gly and MeGly are produced from the gas-phase oxidation of several anthropogenic and biogenic VOCs and could act as a precursor of C_2 via heterogeneous processes (Volkamer et al., 2001; Lim et al., 2005). The dominance of ωC_2 and Gly indicates that they are key precursors of C_2 in Raipur aerosols.

3.3. Size distributions of inorganic ions and methanesulfonic acid

Size distributions of inorganic ions are shown in Fig. 5. The result of correlation analyses among the measured ions in fine and coarse modes is given in Table 2. Na^+ showed bimodal distribution with a large peak in coarse mode and a small peak in fine mode whereas Ca^{2+} and Mg^{2+} showed unimodal distribution with a peak in coarse mode (Fig. 5a-c). Ca^{2+} and Mg^{2+} in coarse mode have frequently been interpreted to be of dust particle origin (Zhuang et al., 1999; Zhao et al., 2011). The similar size distributions and strong correlations between coarse mode Ca^{2+} and Mg^{2+} (r = 0.97) suggest their similar sources and origins probably from dust particles in central India. Good correlation of coarse mode Na^+ with Ca^{2+} (r = 0.70) and Mg^{2+} (r = 0.66) indicate the dust contribution to coarse mode Na^+ in Raipur aerosols. It is noteworthy that Na^+ showed a small peak in fine mode. The fine mode peak of Na^+ may suggest another source of Na^+ in addition to mineral dust in Raipur aerosols. The accumulation of Na^+ in fine mode may be associated with anthropogenic sources such as waste incineration (Kaneyasu et al., 1999).

K^+ showed a bimodal distribution with a major peak in fine mode and a minor peak in coarse mode (Fig. 5d). It is remarkable that fresh biomass burning aerosols derived from crop residues and wood burning had larger mass fraction of K^+ in $D_p < 0.43$ µm (Sang, 2012). Burning of agricultural residues in open field after crop harvesting is common in winter in Raipur and the IGP. The fine mode peak of K^+ in Raipur may be caused by the combination of biomass burning-derived aerosols with secondary aerosol species. It is noteworthy that concentrations of secondary inorganic ions especially SO_4^{2-} and NH_4^+ peaked in the same size range of K^+ in fine mode. A strong correlation of K^+ with SO_4^{2-} (r = 0.85) suggests that fine mode K^+ may be produced by mixing of biomass burning aerosols with anthropogenic aerosols containing substantial amounts of secondary inorganic aerosol precursor such as SO_2 resulted from industrial activities in Raipur and the IGP. The small peak of K^+ in coarse mode shows that there were other sources of K^+ in addition to biomass burning in Raipur. Coarse mode K^+ may be derived from soil resuspension and fertilizers as it showed a strong correlation with Ca^{2+} (r = 0.93).

263 NH_4^+ and SO_4^{2-} showed bimodal distributions with a major peak in fine mode and a minor peak
264 in coarse mode (Fig. 5e and f). NH_4^+ is secondarily produced via heterogeneous reactions of
265 gaseous NH_3 with sulfuric and nitric acids (Seinfeld and Pandis, 1998; Kerminen et al., 2001). Fine
266 mode peak of NH_4^+ may be produced by gas-to-particle conversion via the reaction with sulfuric
267 and nitric acids. Fine mode SO_4^{2-} is produced by homogeneous gas-phase oxidation of SO_2
268 followed by gas-to-particle conversion and oxidation of SO_2 in aerosol aqueous-phase whereas
269 coarse mode SO_4^{2-} could be attributed to a heterogeneous reaction of SO_2 on sea salt and dust
270 particles (Seinfeld and Pandis, 1998). Major peak of SO_4^{2-} in fine mode indicates that most of SO_4^{2-}
271 is produced by aerosol aqueous-phase oxidation of SO_2. The reaction of NH_3 with sulfuric acid or
272 ammonium bisulfate usually favored over its reaction with nitric acid because ammonium sulfate is
273 more stable than ammonium nitrate. Similar size distributions of NH_4^+ and SO_4^{2-}, together with a
274 strong correlation (r = 0.85) between their concentrations in fine mode, suggest that they are
275 internally mixed in the form of ammonium sulfate and ammonium bisulfate.

276 Size distribution of NO_3^- is similar to those of NH_4^+ and SO_4^{2-} (Fig. 5g). The sampling site is a
277 congested area with heavy traffic mainly with diesel trucks and buses as well as cars and double
278 stroke automobiles. The National Highway is approximately 300 m away from the sampling site
279 with heavy vehicular traffic condition of about 25,000 vehicles per day (Deshmukh et al., 2012).
280 These considerations indicate that the major source of NO_3^- in this region may be from traffic
281 emissions (Deshmukh et al., 2010). Moreover, we presume that NO_3^- can also be produced in fine
282 mode from biomass burning. It is noteworthy that biomass burning is commonly occurred in eastern
283 central India during winter (Nirmalkar et al., 2015). NH_4^+ showed a good correlation with NO_3^- (r =
284 0.67) in fine mode. The fine mode NO_3^- can be produced by homogeneous OH radical oxidation of
285 NO_x into nitric acid that reacts with NH_3 to form ammonium nitrate. Russell et al. (1983) suggested
286 that formation of ammonium nitrate is significant at high RH and low temperature. The major fine
287 mode peak of NO_3^- in Raipur aerosols suggests that high RH and low temperature in winter are
288 favorable for the formation of ammonium nitrate in the fine mode. The amounts of gas-phase NH_3

289 also influence the production of NO_3^- in fine and coarse modes. NH_4^+/SO_4^{2-} equivalent ratio varied
290 from 1.0 to 1.5 with an average of 1.3 in fine mode and 1.1 to 2.0 with an average of 1.6 in coarse
291 mode. These results suggest that atmospheric NH_3 was abundant enough to neutralize sulfuric acid
292 and hence NH_4^+ was present in the form of ammonium nitrate in addition to ammonium sulfate in
293 fine and coarse modes.

294 Good correlation of SO_4^{2-} (r = 0.65) and NO_3^- (r = 0.68) with Ca^{2+} was found in coarse mode.
295 This result indicates that coarse mode SO_4^{2-} and NO_3^- is associated with soil dust. Partitioning of
296 nitric acid likely controls the concentration of NO_3^- in coarse mode. Substantial amount of NO_3^-
297 found in coarse mode is likely due to the formation of $Ca(NO_3)_2$ through the reactive adsorption of
298 NO_2 or gas-phase nitric acid onto alkaline dust particles. The coarse mode SO_4^{2-} and NO_3^- is
299 associated with dust and thus coarse mode NH_4^+ may be produced via the heterogeneous reaction of
300 NH_3 with SO_4^{2-} and NO_3^- on dust surface.

301 A bimodal size distribution was observed for MSA^- with a major peak in fine mode and a minor
302 peak in coarse mode (Fig. 5h). MSA^- is produced by the gas- and liquid-phase oxidation of
303 dimethyl sulfide (DMS) (Meinardi et al., 2003). Because biomass burning produces DMS (Meinardi
304 et al., 2003), the peak of MSA in fine mode may be of biomass burning origin. Strong correlations
305 of fine mode MSA^- with K^+ (r = 0.83) and levoglucosan (r = 0.89) suggest that enhanced emission
306 of DMS from biomass burning followed by the subsequent oxidation contributed significantly to
307 fine mode MSA^- in Raipur aerosols. Engling et al. (2009) and Cao et al. (2015) suggested that
308 biomass burning could be a significant source of chloride and chloride-containing compounds in the
309 atmosphere. Cl^- showed a bimodal distribution with a major peak in fine mode and a minor peak in
310 coarse mode (Fig. 5i). The fine mode peak of Cl^- in Raipur aerosols might also be of biomass
311 burning origin. This is also supported by the fact that Cl^- is positively correlated with K^+ or NH_4^+ (r
312 = 0.78) and levoglucosan (r = 0.88) in fine mode. This result suggests that formation of ammonium
313 and potassium chloride is important in fine mode particles via the reaction of NH_3 and K^+ with HCl
314 vapor or chloride-containing compounds produced from combustion sources. It is noteworthy that

315 ammonium chloride salt is stable under the condition of high relative humidity and low
316 temperature.

317 *3.4. Size distributions of WSOC, OC and EC*

318 Size distributions of carbonaceous components are shown in Fig. 6. WSOC showed bimodal
319 distributions with a major peak in fine mode and a minor peak in coarse mode (Fig. 6a). The
320 possible sources of fine mode WSOC include primary emission from combustion sources and
321 secondary photochemical sources (Huang et al., 2006; Ram et al., 2010). WSOC showed a
322 significant positive correlation with K^+ (r = 0.73) in fine mode. Interestingly, levoglucosan, which
323 is a tracer of biomass burning, is also enriched in fine mode (Fig. 6b) and showed a strong
324 correlation (r = 0.92) with WSOC. These results suggest that primary emission from biomass
325 burning or fast oxidation of biomass burning-derived precursors contributed to the production of
326 fine mode WSOC. The minor peak of WSOC was found to be consistent with the same size bin of
327 Ca^{2+} on coarse mode. WSOC was moderately correlated with Ca^{2+} (r = 0.65) in coarse mode. This
328 result suggests that coarse mode WSOC is produced via the adsorption of gaseous organics and
329 oxidation of their anthropogenic and biogenic precursors via heterogeneous reaction on the mineral
330 dust surface.

331 WSOC to OC ratio is a useful parameter to examine the potential sources and photochemical
332 aging of organic aerosols via gas-to-particle formation of secondary WSOC (Miyazaki et al., 2010).
333 The WSOC to OC ratios varied from 0.60 to 0.85 (ave. 0.69±0.07) in fine mode whereas they
334 varied from 0.45 to 0.65 (0.56±0.07) in coarse mode. Higher WSOC to OC ratios (0.5-0.8) were
335 reported in aerosols originated from biomass burning over Amazonia (Mayol-Bracero et al., 2002)
336 and the IGP region (Ram et al., 2010). Higher ratios of WSOC to OC in fine mode suggest that a
337 significant fraction of WSOC was produced from biomass burning in the urban atmosphere of
338 central India.

339 OC and EC showed bimodal distributions with a major peak in fine mode and a minor peak in
340 coarse mode (Fig. 6c and d). OC and EC that are primarily produced from diesel and gasoline

powered vehicles showed maxima in fine mode at or close to the size bin of 0.12 µm whereas those from wood-smoke peaked at 0.12-0.5 µm in diameter (Kleeman et al., 2000; Jaffrezo et al., 2005). The fine mode bins of OC and EC in Raipur aerosols are larger than those produced from diesel and gasoline power vehicles but are comparable or somewhat larger than those of wood-smoke emission. This comparison suggests that fine mode maxima of OC and EC are contributed from biomass burning. EC is primarily produced from combustion process whereas OC is a secondary component produced by photooxidation of VOCs in addition to primary sources. Strong correlations of fine mode OC and EC with K^+ (r = 0.80 and 0.88, respectively) and levoglucosan (0.85 and 0.88, respectively) further support biomass burning as a major source of carbonaceous aerosols in Raipur.

3.5. Size distributions of dicarboxylic acids

The size distributions of selected diacids are shown in Fig. 7. C_2 showed a bimodal distribution with a major peak in fine mode and a minor peak in coarse mode (Fig. 7a). A shift of malonic acid (C_3) peak was found in fine mode at the size of 0.65-1.1 µm. The enhanced presence of C_3 at the size range 0.65-1.1 µm could be likely due to the evaporation of C_3 from smaller-size particles followed by condensation onto larger particles. C_2 can be emitted from primary sources including fossil fuel combustion and biomass burning (Kawamura and Kaplan, 1987; Kundu et al., 2010a; Cong et al., 2015). It can also be secondarily produced by gas-phase and aqueous-phase oxidation of anthropogenic and biogenic VOCs and UFAs (Hatakeyama et al., 1985; Ervens et al., 2004; Carlton et al., 2007; Pavuluri et al., 2015; Zhang et al., 2016a). We found strong correlations of C_2 with K^+ (r = 0.83) and levoglucosan (0.95) in fine mode. This result suggests that primary emission from biomass burning and secondary production from biomass burning-derived precursors are prevalent sources of fine mode C_2 in Raipur aerosols. Similar size distributions and strong positive correlations of other shorter-chain diacids (C_3-C_5) with K^+ (r = 0.81-0.87) and levoglucosan (0.83-0.86) in fine mode also indicate biomass burning as the dominant source.

366 Biomass burning and fossil fuel combustion not only directly produce C_2 but also emit VOCs
367 and UFAs that can be ultimately oxidized to C_2 in the atmosphere. A significant positive correlation
368 of C_2 with SO_4^{2-} (r = 0.65) in fine mode indicates the secondary production of C_2 in Raipur
369 aerosols. C_2 can be produced by the oxidation of longer-chain diacids (C_2-C_9) in aqueous-phase
370 (Legrand et al., 2007; Pavuluri et al., 2015). Interestingly, we found strong correlations (r = 0.80-
371 0.93) among C_2-C_9 diacids in fine mode. This result indicates that they might have similar sources
372 or C_2 may be produced in fine mode via the decay of its higher homologues, that is, C_3-C_9 diacids.
373 ωC_2 is a key intermediate to produce C_2 in aqueous-phase (Lim et al., 2005; Legrand et al., 2007).
374 A strong correlation of C_2 with ωC_2 (r = 0.91) suggests that they may have similar sources and
375 formation processes or C_2 may be produced by the oxidation of ωC_2 in fine mode.

376 C_3 to C_4 ratio can be used as a parameter to evaluate the photochemical processing of organic
377 aerosols because C_4 tends to be degraded into C_3. Average C_3/C_4 ratios in size-segregated aerosols
378 in Raipur ranged from 0.12 to 0.45 (Figure 8a). These values are much lower than those from
379 remote marine aerosols over the North and equatorial Pacific (ave. 3.9, Kawamura and Sakaguchi,
380 1999). C_3/C_4 ratios in Raipur aerosols were even lower than those of winter aerosols in India (1.5,
381 Pavuluri et al., 2010), China (1.1, Wu et al., 2015), Hong Kong (1.3, Ho et al., 2006), Gosan Jeju
382 Island (1.2, Kundu et al., 2010b), and Chichijima Island (1.2, Mochida et al., 2003), where aerosols
383 were seriously subjected to photochemical transformation. Lower C_3/C_4 ratios were usually found
384 in freshly produced aerosols from wood burning (0.12, Wu et al. 2015), fossil fuel combustion
385 (0.35, Kawamura and Kaplan, 1987), and biomass burning derived aerosols from Mt. Everest (0.51,
386 Cong et al., 2015) and Brazil (0.66, Kundu et al., 2010a). The lower ratios suggest that aerosols
387 from Raipur were freshly emitted from biomass burning and biofuel combustion without serious
388 photooxidation.

389 Maleic acid (M) is produced by the photooxidation of aromatic hydrocarbons such as benzene
390 and toluene derived from combustion sources. Kawamura and Sakaguchi (1999) proposed that *cis*
391 *configuration* (M) could be isomerized to *trans* fumaric acid (F) under the solar radiation through

photochemical processes. Average F/M ratios in size-segregated aerosols (0.23-0.31) in Raipur (Figure 8b) are much lower than those from the marine aerosols from the North Pacific (3.2, Kawamura and Sakaguchi, 1999). This comparison suggests that photochemical processing in Raipur is not as significant as in marine aerosols. It is of interest to note that F/M ratios in Raipur aerosols are comparable to those from the urban aerosols from India (0.35, Miyazaki et al., 2009), Hong Kong (0.15, Ho et al., 2006), and biomass burning derived aerosols from Brazil (0.37, Kundu et al., 2010a). The lower ratios further suggest that Raipur aerosols were rather fresh originating from biomass burning and biofuel combustion.

Considerable amount of C_2 was detected in coarse mode (Table 1). The peak of C_2 in coarse mode appeared exactly in the same size fraction with Ca^{2+}. Coarse mode C_2 showed good correlation with Ca^{2+} (r = 0.63). This result suggests that coarse mode C_2 is associated with dust particles. A substantial fraction of C_2 in coarse mode may also be derived from gas-phase oxidation of organic acids and their precursors in central India. C_2 showed a good correlation with coarse mode NO_3^- (r = 0.68), which is preferentially produced in calcium-rich dust particles via the oxidation of their gaseous precursors on calcium carbonate particles. A good correlation between C_2 and NO_3^- suggests that C_2 and its precursors was experiencing similar formation processes with NO_3^- in coarse mode. Coarse mode C_2 was likely produced by uptake of gaseous C_2 diacid and heterogeneous reaction of C_2 precursors onto alkaline dust particles.

C_9 diacid showed bimodal distribution with peaks in fine and coarse modes. C_9 is strongly correlated with K^+ (r = 0.93) in fine mode. Interestingly, a strong correlation was also found between C_9 and levoglucosan (r = 0.98) in fine mode. This result suggests that C_9 diacid may be directly emitted into the atmosphere from biomass burning in fine mode. Huang et al. (2005) and Tedetti et al. (2007) suggested that C_9 is also produced via the oxidation of UFAs such as oleic acid ($C_{18:1}$) having a double bond at C-9 position. It is noteworthy that biomass burning can also produce oleic acid abundantly (Hays et al., 2005). Therefore, the peak of C_9 in fine mode may also be produced by the oxidation of UFAs of biomass burning origin in Raipur. High correlation of C_9

418 with SO_4^{2-} (r = 0.83) in fine mode also suggests that secondary photochemical production
419 contributed significantly to fine mode C_9 in Raipur aerosols. A positive correlation of C_9 was found
420 with Ca^{2+} (r = 0.65) and Mg^{2+} (r = 0.63) in coarse mode. Coarse mode C_9 can be produced by the
421 heterogeneous oxidation of UFAs possibly on the surface of dust particles.

422 Ph or tPh is the second or third most abundant diacids in Raipur aerosols (Fig. 7g and h). Ph
423 showed a large peak in coarse mode and a small peak in fine mode whereas tPh showed an opposite
424 trend. It is noteworthy that Ph and its precursor (naphthalene) usually exist in the gas-phase
425 (Schauer et al., 1996). A larger peak of Ph in coarse mode is due to an enhanced adsorption of
426 gaseous Ph as well as oxidation of its precursors in gas-phase followed by adsorption on the surface
427 of alkaline dust particles in coarse mode. tPh is mostly produced by the burning of plastic bags and
428 bottles (Simoneit et al., 2005; Kawamura and Pavuluri, 2010), and then deposited on the pre-
429 existing fine particles.

430 Molecular compositions of diacids can be used as tracer of source strength of organic aerosols.
431 C_6/C_9 and Ph/C_9 ratios are useful tracers to evaluate anthropogenic vs. biogenic contributions to
432 diacids because C_6 and Ph are produced by the oxidation of anthropogenic cyclohexene and
433 aromatic hydrocarbons (Hatakeyama et al., 1985; Kawamura and Ikushima, 1993), respectively
434 whereas C_9 is produced by the oxidation of biogenic UFAs (Kawamura and Gagosian, 1987; Tedetti
435 et al., 2007). The average C_6/C_9 ratios in size-segregated aerosols in Raipur (0.10-0.26) is much
436 lower than those reported for Gosan Jeju Island (1.4, Kundu et al., 2010b) and Chichijima Island
437 (3.2, Mochida et al., 2003), where anthropogenic sources was the major source of organic acids.
438 Average Ph/C_9 ratios in size-segregated aerosols in Raipur (0.69-0.98) are lower than those reported
439 in India (1.0-2.0, Pavuluri et al., 2010), China (1.8, Wang et al., 2012), Hong Kong (5.2, Ho et al.,
440 2006), Mongolia (1.3, Jung et al., 2010), Gosan Jeju Island (5.6, Kundu et al., 2010b), and Chichi-
441 jima Island (8.9, Mochida et al., 2003). These comparisons suggest that Raipur aerosols are more
442 influenced from biogenic UFAs possibly derived from biomass burning. Biomass burning is usually

443 considered as anthropogenic sources but the materials are mostly of biogenic origin and thus C_9 is
444 produced by the oxidation of biogenic UFAs.

445 *3.6. Size distributions of ω-oxoacids and pyruvic acid*

446 Size distributions of ω-oxoacids and pyruvic acid are shown in Fig. 9. ωC_2 showed a bimodal
447 distribution with a major peak in fine mode and a minor peak in coarse mode. Fine mode maxima of
448 ωC_2 suggest that this oxoacid is primarily produced from biofuel and biomass burning and
449 secondarily produced in the atmosphere via photooxidation of organic precursors in fine size
450 fractions. This is further supported by the fact that ωC_2 was strongly correlated with K^+ ($r = 0.81$)
451 and levoglucosan ($r = 0.90$) in fine mode. Gly and MeGly are the precursors of ωC_2 in aerosols via
452 aqueous-phase processing (Lim et al., 2005; Myriokefalitakis et al., 2011). ωC_2 was significantly
453 correlated with Gly ($r = 0.85$) whereas a weak correlation was found with MeGly (0.53) in fine
454 mode. This result suggests that Gly is a main precursor of ωC_2 in fine mode.

455 The gas-phase and aqueous-phase processing of ω-oxoacids with $OH^{\bullet}$ produces diacids in the
456 atmosphere (Carlton et al., 2007; Wang et al., 2012; Pavuluri et al., 2015; Zhang et al., 2016b).
457 Strong correlations ($r = 0.82$-0.91) of fine mode C_2-C_5 ω-oxoacids with corresponding diacids (C_2-
458 C_5) suggest that both ω-oxoacids and diacids are simultaneously produced in fine mode from
459 similar sources and atmospheric processes possibly via gas- and aqueous-phase oxidation of their
460 precursors derived from combustion sources. These high correlations further suggest that diacids
461 are produced by the oxidation of corresponding ω-oxoacids in fine mode. Coarse mode peak of ωC_2
462 in the same size bin of Ca^{2+} shows that this oxoacid is associated with mineral dust. A substantial
463 fraction of ωC_2 in coarse mode (Table 1) may be produced through the accumulation of gaseous
464 ωC_2 originated from combustion sources and heterogeneous oxidation of their precursors on dust
465 particles. A positive correlation of ωC_2 and Gly ($r = 0.63$) indicates that gas-phase and aerosol-
466 phase Gly may undergo heterogeneous oxidation to produce ωC_2 on coarse mode particles.

467 9-Oxononanoic acid (ωC_9) showed a bimodal distribution with peaks in fine and coarse mode
468 (Figure 9). ωC_9 is produced by the oxidation of UFAs such as oleic acid ($C_{18:1}$) and further oxidized

469 to C_9 in the atmosphere (Kawamura and Gagosian, 1987; Ziemann, 2005). Positive correlations of
470 ωC_9 with C_9 (r = 0.62) and levoglucosan (0.80) in fine mode suggest that UFAs produced by
471 biomass burning undergo photooxidation to produce ωC_9 in fine mode. The peak of ωC_9 in coarse
472 mode suggests that oxidation of UFAs probably occurs via heterogeneous reaction on dust particles.
473 Based on the above observation together with high abundance of C_9 suggests that photooxidation of
474 UFAs originated from biomass burning could be a major source of these species in central India.
475 Pyruvic acid showed bimodal distributions with a major peak in fine mode and minor peak in
476 coarse mode. Lim et al. (2005) and Carlton et al. (2006) proposed that anthropogenic and biogenic
477 VOCs form MeGly in gas-phase that can be hydrated in aqueous-phase to form pyruvic acid in the
478 atmosphere. The fine mode peak of pyruvic acid suggests gaseous oxidation of anthropogenic
479 VOCs whereas coarse mode peak suggests its origin via heterogeneous oxidation of organic
480 precursors on dust particles.

481 *3.7. Size distributions of α-dicarbonyls*

482 Gly and MeGly are gas-phase oxidation products of VOCs including benzene and toluene
483 (Legrand et al., 2007), xylene (Volkamer et al., 2001) as well as ethylene and isoprene
484 (Zimmermann and Poppe, 1996; Lim et al., 2005). They have received much attention because their
485 aqueous-phase oxidation is the global and regional source of SOA including C_2 (Warneck, 2003;
486 Carlton et al., 2007). Gly and MeGly showed bimodal distribution with nearly equal size of peaks in
487 fine and coarse modes (Figure 10). Photooxidation of aromatic hydrocarbons produced from
488 combustion sources has been proposed as a major source of Gly and MeGly in urban areas (Hays et
489 al., 2002; Fu et al., 2008; Jung et al., 2010). Fine mode Gly is strongly correlated with K^+ and
490 levoglucosan (r = 0.86 and 0.92, respectively) whereas MeGly showed moderate correlation (0.59
491 and 0.60, respectively). These results suggest that biomass burning is a major source of fine mode
492 Gly in Raipur aerosols.

493 Gly and MeGly showed peaks on coarse mode that are comparable to peaks in fine mode. The
494 coarse mode peaks of Gly and MeGly appeared in the size bin of Ca^{2+}. Moderate correlations of

Gly (r = 0.63) and MeGly (0.59) were also found with Ca^{2+} in coarse mode. This result suggests that coarse mode Gly and MeGly are associated with mineral dust in Raipur. The considerable fraction of Gly and MeGly in coarse mode provides an evidence of their major gas-phase precursors in Raipur region. Coarse mode Gly and MeGly may be produced via the adsorption of gas-phase Gly and MeGly as well as partitioning of their gaseous precursors on the surface of mineral dust followed by heterogeneous oxidation.

Gly and MeGly are mostly present in gas-phase and only small portion is in aerosols (Kawamura et al., 2013). Gly and MeGly are a crucial SOA_{aq} precursor. They are highly water-soluble and reactive to OH radical and can diffuse into aerosol where it is converted to SOA through formation of low volatility products such as organic acids and oligomers (Warneck, 2003; Carlton et al., 2006). Thus, considerable fractions of Gly and MeGly in coarse mode aerosols in Raipur are crucial in terms of heterogeneous oxidation to result in ωC_2 and C_2 (Lim et al., 2005; Wang et al., 2012), which have a significant influence on chemical and physical properties of urban aerosols. SOA_{aq} are generally essential components of fine particles. Their association with coarse mode aerosols via the uptake of gaseous Gly and MeGly or heterogeneous reaction of anthropogenic and biogenic precursors on mineral dust surface can alter their residence time and may suppress the formation of SOA_{aq} in fine mode due to the decrease in the abundance of precursors. These processes may thus reduce the contribution of SOA_{aq} to light scattering and cloud droplet formation because they are sensitive to the number and mass concentrations of fine particles.

4. Summary and conclusions

Size-segregated aerosols in 9-size fractions were collected in the urban atmosphere of Raipur, central India in winter of 2012-2013 and analyzed for diacids and related compounds as well as carbonaceous components and inorganic ions to investigate their sources and formation mechanism. Diacids showed a predominance of oxalic acid (C_2) followed by succinic and azelaic (C_9) acid whereas ω-oxoacids showed a predominance of glyoxylic acid and glyoxal was the most abundant α-dicarbonyl in all the sizes. High abundance of C_9 demonstrates its unique source of UFAs

associated with the emission from biomass burning and the subsequent oxidation to C_9 in central India.

Diacids, ω-oxoacids and α-dicarbonyls showed bimodal distributions with peaks in fine and coarse modes. SO_4^{2-}, NO_3^-, NH_4^+ and K^+ showed bimodal distributions with a major peak in fine mode and minor peak in coarse mode whereas Ca^{2+} and Mg^{2+} showed unimodal distribution with a peak in coarse mode. Strong correlations of diacids and related compounds with K^+ and levoglucosan in fine mode suggest a significant contribution of primary emission from biomass burning and secondary production from biomass burning-derived precursors. Similar size distributions and strong correlations among normal-chain diacids (C_2-C_9) in fine mode suggest their similar sources with a strong link to photochemical chain reactions to produce C_2 by the oxidation of longer-chain diacids. Substantial fractions of diacids and related compounds in coarse mode are likely associated with dust particles via the uptake of gaseous diacids and related compounds and with the oxidation of anthropogenic and biogenic precursors via heterogeneous reaction on alkaline dust particles. This study denoted that biomass burning and mineral dust particles are largely involved with the size distributions of diacids and related compounds in the urban atmosphere over central India.

Acknowledgements

We acknowledge the financial support from the Japan Society for the Promotion of Science (JSPS) through Grant-in-Aid No. 24221001. The authors greatly appreciate the National Oceanic and Atmospheric Administration (NOAA) Air Resources Laboratory for the provision of the Hybrid Single-Particle Lagrangian Integrated Trajectory model 4.0 for seven-day air mass backward trajectory at the observation site during the study period. We appreciate the financial support of a JSPS fellowship to D. K. Deshmukh.

References

Agarwal, S., Aggarwal, S.G., Okuzawa, K., Kawamura, K., 2010. Size distributions of dicarboxylic acids, ketoacids, alpha-dicarbonyls, sugars, WSOC, OC, EC and inorganic ions in atmospheric particles over Northern Japan: implication for long-range transport of Siberian biomass burning and East Asian polluted aerosols. Atmos. Chem. Phys. 10, 5839-5858.

Cao, F., Zhang, S.C., Kawamura, K., Zhang, Y.L., 2015. Inorganic markers, carbonaceous components and stable carbon isotop from biomass burning aerosols in Northeast China. Sci. Total Environ., doi:10.1016/j.scitotenv.2015.09.099.

Carlton, A.G., Turpin, B.J., Altieri, K.E., Seitzinger, S., Reff, A., Lim, H.J., 2007. Atmospheric oxalic acid and SOA production from glyoxal: results of aqueous photooxidation experiments. Atmos. Environ. 41, 7588-7602.

Carlton, A.G., Turpin, B.J., Lim, H.J., Altieri, K.E., Seitzinger, S., 2006. Link between isoprene and secondary organic aerosol (SOA): pyruvic acid oxidation yields low volatility organic acids in clouds. Geophys. Res. Lett. 33, L06822, doi:10.1029/2005GL025374.

Chebbi, A., Carlier, P., 1996. Carboxylic acids in the troposphere, occurrence, sources, and sinks: a review. Atmos. Environ. 30, 4233-4249.

Chowdhury, Z., Zheng, M., Schauer, J.J., Sheesley, R.J., Salmon, L., Cass, G.R., 2007. Speciation of ambient fine organic carbon particles and source apportionment of $PM_{2.5}$ in Indian cities. J. Geophys. Res. 112, D15303, doi:10.1029/2007JD008386.

Cong, Z., Kawamura, K., Kang, S., Fu, P., 2015. Penetration of biomass-burning emissions from South Asia through the Himalayas: new insights from atmospheric organic acids. Sci. report 5, 9580, doi:10.1038/SREP09580.

Davidson, C.I., Phalen, R.F., Solomon, P.A., 2005. Airborne particulate matter and human health: A review. Aerosol Sci. Technol. 39, 737-749.

Deshmukh, D.K., Deb, M.K., Tsai, Y.I., Mkoma, S.L., 2010. Atmospheric ionic species in $PM_{2.5}$ and PM_1 aerosols in the ambient air of eastern central India. J. Atmos. Chem. 66, 81-100.

Deshmukh, D.K., Tsai, Y.I., Deb, M.K., Mkoma, S.L., 2012. Characterization of dicarboxylates and inorganic ions in urban PM_{10} aerosols in the eastern central India. Aerosol Air Qual. Res. 12, 592-607.

Deshmukh, D.K., Deb, M.K., Suzuki, Y., Kouvarakis, G.N., 2013. Water-soluble ionic composition of $PM_{2.5\text{-}10}$ and $PM_{2.5}$ aerosols in the lower troposphere of an industrial city Raipur, the eastern central India. Air Qual. Atmos. Health 6, 95-110.

Draxler, R.R.R., Rolph, G.D., 2013. HYbrid Single–Particle Lagrangian Integrated Trajectory Model, access via NOAA ARL READY website available at: http://www.arl.noaa.gov/HYSPLIT.php 2013 (last access: 05 Januarry 2015), NOAA Air Resources Laboratory, College Park, MD.

Engling, G., Lee, J.J., Tsai, Y.W., Lung, S.C.C., Chou, C.C.K., Chan, C.Y., 2009. Size-resolved anhydrosugar composition in smoke aerosol from controlled field burning of rice straw. Aerosol Sci. Technol. 43, 662-672.

Enami, S., Hoffmann, M.R., Colussi, A.J., 2015. Stepwise oxidation of aqueous dicarboxylic acids by gas-phase OH radicals. J. Phys. Chem. Lett. 6, 527-534.

Ervens B., Feingold, G., Frost, G.J., Kredenweis, S.M., 2004. A modeling study of aqueous production of dicarboxylic acids: 1. chemical pathways and speciated organic mass production. J. Geophys. Res., 109, D15205, doi:10.1029/2003JD004387.

588 Falkovich, A.H., Graber, E.R., Schkolnik, G., Rudich, Y., Maenhaut, W., Artaxo, P., 2005. Low
589 molecular weight organic acids in aerosol particles from Rondonia, Brazil, during the
590 biomass-burning, transition and wet periods. Atmos. Chem. Phys. 5, 781-797.

591 Fu, T.-M., Jacob, D.J., Wittrock, F., Burrows, J.P., Vrekoussis, M., Henze, D.K., 2008. Global
592 budgets of atmospheric glyoxal and methylglyoxal, and applications for formation of
593 secondary organic aerosols. J. Geophys. Res. 113, D15303, doi:10.1029/2007JD009505.

594 Fu, P.Q., Kawamura, K., Pavuluri, C.M., Swaminathan, T., Chen, J., 2010. Molecular
595 characterization of urban organic aerosol in tropical India: contributions of primary
596 emissions and secondary photooxidation. Atmos. Chem. Phys. 10, 2663-2689.

597 Fu, P.Q., Kawamura, K., Usukura, K., Miura, K., 2013. Dicarboxylic acids, ketocarboxylic acids
598 and glyoxal in the marine aerosols collected during a round-the-world cruise. Marine Chem.
599 148, 22-32.

600 Gustafsson, O., Krusa, M., Zencak, Z., Sheesley, R.J., Granat, L., Engstrom, E., 2009. Brown
601 clouds over South Asia: biomass or fossil fuel combustion? Science 323, 495-498.

602 Hatakeyama, S., Tanonaka, T., Weng, J.H., Bandow, H., Takagi, H., Akimoto, H., 1985. Ozone
603 cyclohexene reaction in air - quantitative-analysis of particulate products and the reaction-
604 mechanism. Environ. Sci. Technol. 19, 935-942.

605 Hays, M.D., Fine, P.M., Geron, C.D., Kleeman, M.J., Gullett, B.K., 2005. Open burning of
606 agricultural biomass: physical and chemical properties of particle-phase emissions. Atmos.
607 Environ. 39, 6747-6764.

608 Hays, M.D., Geron, C.D., Linna, K.J., Smith, N.D., Schauer, J.J., 2002. Speciation of gas-phase and
609 fine particle emissions from burning of foliar fuels. Environ. Sci. Technol. 36, 2281-2295.

610 Hegde, P., Kawamura, K., 2012. Seasonal variations of water-soluble organic carbon, dicarboxylic
611 acids, ketocarboxylic acids, and alpha-dicarbonyls in Central Himalayan aerosols. Atmos.
612 Chem. Phys. 12, 6645-6665.

613 Ho, K.F., Lee, S.C., Cao, J.J., Kawamura, K., Watanabe, T., Cheng, Y., 2006. Dicarboxylic acids,
614 ketocarboxylic acids and dicarbonyls in the urban roadside area of Hong Kong. Atmos.
615 Environ. 40, 3030-3040.

616 Ho, K.F., Cao, J.J., Lee, S.C., Kawamura, K., Zhang, R.J., Chow, J.C., Watson, J.G., 2007.
617 Dicarboxylic acids, ketocarboxylic acids, and dicarbonyls in the urban atmosphere of China,
618 J. Geophys. Res., 112, D22S27, doi:10.1029/2006jd008011.

619 Huang, H.M., Katrib, Y., Martin, S.C., 2005. Products and mechanisms of the reaction of oleic acid
620 with ozone and nitrate radical. J. Phys. Chem. A, 109, 4517-4530.

621 Huang, X.F., Yu, J.Z., He, L.Y., Yuan, Z.B., 2006. Water-soluble organic carbon and oxalate in
622 aerosols at a coastal urban site in China: Size distribution characteristics, sources, and
623 formation mechanisms. J. Geophys. Res. 111, D22212, doi:10.1029/2006JD007408.

624 Jaffrezo, J.-L., Aymoz, G., Cozic, J., 2005. Size distribution of EC and OC in the aerosol of Alpine
625 valleys during summer and winter. Atmos. Chem. Phys. 5, 2915-2925.

626 Jung, J.S., Tsatsral, B., Kim, Y.J., Kawamura, K., 2010. Organic and inorganic aerosol
627 compositions in Ulaanbaatar, Mongolia, during the cold winter of 2007 to 2008:
628 Dicarboxylic acids, ketocarboxylic acids, and alpha-dicarbonyls. J. Geophys. Res. 115,
629 D22203, doi:10.1029/2010JD014339.

630 Kanakidou, M., Seinfeld, J.H., Pandis, S.N., Barnes, I., Dentener, F.J., Facchini, M.C., et al. 2005.
631 Organic aerosol and global climate modelling: a review. Atmos. Chem. Phys. 5, 1053-1123.

632 Kaneyasu, N., Yoshikado, H., Mizuno, T., Sakamoto, K., Soufuku, M., 1999. Chemical forms and
633 sources of extremely high nitrate and chloride in winter aerosol pollution in the Kanto Plain
634 of Japan. Atmos. Environ. 33, 1745-1756.

635 Kawamura, K., Gagosian, R.B., 1987. Implications of ω-oxocarboxylic acids in the remote marine
636 atmosphere for photo-oxidation of unsaturated fatty acids. Nature 325, 330-332.

637 Kawamura, K., Ikushima, K., 1993. Seasonal changes in the distribution of dicarboxylic acids in the
638 urban atmosphere. Environ. Sci. Technol. 27, 2227-2235.

639 Kawamura, K., Kaplan, I.R., 1985. Motor exhaust emissions as a primary source for dicarboxylic-
640 acids in Los-Angeles ambient air. Environ. Sci. Technol. 21, 105-110.

641 Kawamura, K., 1993. Identification of C_2-C_{10} ω-oxocarboxylic acids, pyruvic acid, and C_2-C_3 α-
642 dicarbonyls in wet precipitation and aerosol samples by capillary GC and GC/MS. Anal.
643 Chem. 65, 3505-3511.

644 Kawamura, K., Kasukabe, H., Barrie, L.A., 1996a. Source and reaction pathways of dicarboxylic
645 acids, ketoacids and dicarbonyls in arctic aerosols: one year of observations. Atmos.
646 Environ. 30, 1709-1722.

647 Kawamura, K., Sempéré, R., Imai, Y., Fujii, Y., Hayashi, M., 1996b. Water soluble dicarboxylic
648 acids and related compounds in Antarctic aerosols. J. Geophys. Res. 101, 18721-18728.

649 Kawamura, K., Pavuluri, C.M., 2010. New Directions: Need for better understanding of plastic
650 waste burning as inferred from high abundance of terephthalic acid in South Asian aerosols.
651 Atmos. Environ. 44, 5320-5321.

652 Kawamura, K., Sakaguchi, F., 1999. Molecular distributions of water soluble dicarboxylic acids in
653 marine aerosols over the Pacific Ocean including tropics. J. Geophys. Res. 104, 3501-3509.

654 Kawamura, K., Tachibana, E., Okuzawa, K., Aggarwal, S.G., Kanaya, Y., Wang, Z.F., 2013. High
655 abundances of water-soluble dicarboxylic acids, ketocarboxylic acids and ・-dicarbonyls in
656 the mountaintop aerosols over the North China Plain during wheat burning season. Atmos.
657 Chem. Phys. 13, 8285-8302.

658 Kawamura, K., Yasui, O., 2005. Diurnal changes in the distribution of dicarboxylic acids,
659 ketocarboxylic acids and dicarbonyls in the urban Tokyo atmosphere. Atmos. Environ. 39,
660 1945-1960.

661 Kawamura, K., and Bikkina, S., 2016. A review of dicarboxylic acids and related compounds in
662 atmospheric aerosols: Molecular distributions, sources and transformation, Atmos. Res.,
663 170, 140-160.

664 Kerminen, V.-M., Teinila, K., Hillamo, R., Makela, T., 1999. Size-segregated chemistry of
665 particulate dicarboxylic acids in Arctic atmosphere. Atmos. Environ. 33, 2089-2100.

666 Kerminen, V.-M., Hillamo, R., Teinilä, K., Pakkanen, T., Allegrini, I., Sparapani, R., 2001. Ion
667 balances of size-resolved tropospheric aerosol samples: implications for the acidity and
668 atmospheric processing of aerosols. Atmos. Environ. 35, 5255-5265.

669 Kleeman, M.J., Schauer, J.J., Cass, G.R., 2000. Size and composition distribution of fine particulate
670 matter emitted from motor vehicles. Environ. Sci. Technol. 34, 1132-1142.

671 Kundu, S., Kawamura, K., Andreae, T.W., Hoffer, A., Andreae, M.O., 2010a. Molecular
672 distributions of dicarboxylic acids, ketocarboxylic acids and α-dicarbonyls in biomass
673 burning aerosols: implications for photochemical production and degradation in smoke
674 layers. Atmos. Chem. Phys. 10, 2209-2225.

675 Kundu, S., Kawamura, K., Lee, M., 2010b. Seasonal variations of diacids, ketoacids, and α-
676 dicarbonyls in aerosols at Gosan, Jeju Island, South Korea: implications for sources,

formation, and degradation during long-range transport. J. Geophys. Res. 115, D19307, doi:10.1029/2010JD013973.

Legrand, M., Preunkert, S., Oliveira, T., Pio, C.A., Hammer, S., Gelencser, A., et al. 2007. Origin of C_2-C_5 dicarboxylic acids in the European atmosphere inferred from year-round aerosol study conducted at a west-east transect. J. Geophys. Res. 112, D23S07, doi:10.1029/2006JD008019.

Lim, H.J., Carlton, A.G., Turpin, B.J., 2005. Isoprene forms secondary organic aerosol through cloud processing: model simulations. Environ. Sci. Technol. 39, 4441-4446.

Mayol-Bracero, O.L., Guyon, P., Graham, B., Roberts, G., Andreae, M.O., Decesari, S., Facchini, M.C., Fuzzi, S., Artaxo, P., 2002. Water-soluble organic compounds in biomass burning aerosols over Amazonia - 2. apportionment of the chemical composition and importance of the polyacidic fraction. J. Geophys. Res. 107, 8091, doi:10.1029/2001JD000522.

Meinardi, S., Simpson, I.J., Blake, N.J., Blake, D.R., Rowland, F.S., 2003, Dimethyl disulfide (DMDS) and dimethyl sulfide (DMS) emissions from biomass burning in Australia. Geophys Res Lett 30, 1454, doi:10.1029/2003GL016967.

Miyazaki, Y., Aggarwal, S.G., Singh, K., Gupta, P.K., Kawamura, K., 2009. Dicarboxylic acids and water-soluble organic carbon in aerosols in New Delhi, India, in winter: characteristics and formation processes. J. Geophys. Res. 114, D19206, doi:10.1029/2009JD011790.

Miyazaki, Y., Kawamura, K., Jung, J., Furutani, H., Uematsu, M., 2011. Latitudinal distributions of organic nitrogen and organic carbon in marine aerosols over the western North Pacific. Atmos. Chem. Phys. 11, 3037-3049.

Miyazaki, Y., Kawamura, K., Sawano, M., 2010. Size distributions and chemical characterization of water-soluble organic aerosols over the western North Pacific in summer. J. Geophys. Res. 115, D23210, doi: 10.1029/2010JD014439.

Mkoma, M., Kawamura, K., 2013. Molecular composition of dicarboxylic acids, ketocarboxylic acids, α-dicarbonyls and fatty acids in atmospheric aerosols from Tanzania, East Africa during wet and fry seasons. Atmos. Chem. Phys. 13, 2235-2251.

Mochida, M., Kawabata, A., Kawamura, K., Hatsushika, H., Yamazaki, K., 2003. Seasonal variation and origins of dicarboxylic acids in the marine atmosphere over the western North Pacific. J. Geophys. Res. 108, 4193, doi:10.10.29/2002JD002355.

Mochida, M., Umemoto, N., Kawamura, K., Lim, H.-J., Turpin, B.J., 2007. Bimodal size distributions of various organic acids and fatty acids in the marine atmosphere: influence of anthropogenic aerosols, Asian dusts, and sea spray off the coast of East Asia. J. Geophys. Res. 112, D15209, doi:10.1029/2006JD007773.

Myriokefalitakis, S., Tsigaridis, K., Mihalopoulos, N., Sciare, J., Nenes, A., Kawamura, K., et al. 2011. In-cloud oxalate formation in the global troposphere: a 3-D modeling study. Atmos. Chem. Phys. 11, 5761-5782.

Niranjan, K., Sreekanth, V., Madhavan, B.L., Moorthy, K.K., 2006. Wintertime aerosol characteristics at a north Indian site Kharagpur in the Indo-Gangetic plains located at the outflow region into Bay of Bengal. J. Geophys. Res. 111, D24209, doi:10.1029/2006JD007635.

Nirmalkar, J., Deshmukh, D.K., Deb, M.K., Tsai, Y.I., Sopajaree, K., 2015. Mass loading and episodic variation of molecular markers in $PM_{2.5}$ aerosols over a rural area in eastern central India. Atmos. Environ. 117, 41-50.

721 Pant, P., Baker, S.J., Goel, R., Guttikunda, S., Goel, A., Shukla, A., Harrison, R.M., 2016. Analysis
722 of size-segregated winter season aeosol data from New Delhi, India. Atmos. Poll. Res. 7,
723 100-109.

724 Pavuluri, C.M., Kawamura, K., Mihalopoulos, N., Swaminathan, T., 2015. Laboratory
725 photochemical processing of aqueous aerosols: formation and degradation of dicarboxylic
726 acids, oxocarboxylic acids and alpha-dicarbonyls. Atmos. Chem. Phys. 15, 7999-8012.

727 Pavuluri, C.M., Kawamura, K., Swaminathan, T., 2010. Water-soluble organic carbon, dicarboxylic
728 acids, ketoacids, and alpha-dicarbonyls in the tropical Indian aerosols. J. Geophys. Res. 115,
729 D11302, doi:10.1029/2009JD012661.

730 Prenni, A.J., De Mott, P.J., Kreidenweis, S.M., 2003. Water uptake of internally mixed particles
731 containing ammonium sulfate and dicarboxylic acids. Atmos. Environ. 37, 4243-4251.

732 Ram, K., Sarin, M.M., Tripathi, S.N., 2010. A 1 year record of carbonaceous aerosols from an
733 urban site in the Indo-Gangetic Plain: characterization, sources, and temporal variability. J.
734 Geophys. Res. 115, D24313, doi:10.1029/2010JD014188.

735 Ramanathan, V., Ramana, M.V., Roberts, G., Kim, D., Corrigan, C., Chung, C., et al. 2007.
736 Warming trends in Asia amplified by brown cloud solar absorption. Nature 448, 575-578.

737 Russell, A.G., McRae, G.J., Cass, G.R., 1983. Mathematical modeling of the formation and
738 transport of ammonium nitrate aerosol. Atmos. Environ. 17, 949-964.

739 Sang, X.F., 2012. Carbon isotope and size distributions of biomass burning aerosols and their
740 influence to atmospheric environment. Sun Yat-sen University, China.

741 Schauer, J.J., Rogge, W.F., Hildemann, L.M., Mazurek, M.A., Cass, G.R., 1996. Source
742 apportionment of airborne particulate matter using organic compounds as tracers. Atmos.
743 Environ. 30, 3837-3855.

744 Seinfeld, J.H., Pandis, S.N., 1998. Atmospheric Chemistry and Physics. New York: John Wiley &
745 Sons.

746 Simoneit, B.R.T., Schauer, J.J., Nolte, C.G., Oros, D.R., Elias, V.O., Fraser, M.P., Rogge, W.F.,
747 Cass, G.R., 1999. Levoglucosan, a tracer for cellulose in biomass burning and atmospheric
748 particles. Atmos. Environ. 33, 173-182.

749 Simoneit, B.R.T., Medeiros, P.M., Didyk, B.M., 2005. Combustion products of plastics as
750 indicators for refuse burning in the atmosphere. Environ. Sci. Technol. 39, 6961-6970.

751 Tedetti, M., Kawamura, K., Narukawa, M., Joux, F., Charriere, B., Sempéré, R., 2007. Hydroxyl
752 radical-induced photochemical formation of dicarboxylic acids from unsaturated fatty acids
753 (oleic acid) in aqueous solution. J. Photochem. Photobiol. A 188, 135-139.

754 Tremblay, R.T., Riemer, D.D., Zika, R.G., 2007. Organic composition of $PM_{2.5}$ and size-segregated
755 aerosols and their sources during the 2002 Bay Regional Atmospheric Chemistry
756 Experiment (BRACE), Florida, USA. Atmos. Environ. 41, 4323-4335.

757 Tsai, Y.I., Kuo, S.C., 2013. Contributions of low molecular weight carboxylic acids to aerosols and
758 wet deposition in a natural subtropical broad-leaved forest environment. Atmos. Environ.
759 81, 270-297

760 Turpin, B.J., Lim, H.J., 2001. Species contributions to $PM_{2.5}$ mass concentrations: Revisiting
761 common assumptions for estimating organic mass. Aerosol Sci. Technol. 35, 602-610.

762 Turpin, B.J., Saxena, P., Andrews, E., 2000. Measuring and simulating particulate organics in the
763 atmosphere: problems and prospects. Atmos. Environ. 34, 2983-3013.

764 Van Pinxteren, D., Neususs, C., Hermann, H., 2014. On the abundnace and source contributions of
765 dicarboxylic acids in size-resolved aerosol particles at continental sites in central Europe.
766 Atmos. Chem. Phys. 14, 3913-3928.

767 Verma, S.K., Deb, M.K., Suzuki, Y., Tsai, Y.I., 2010. Ion chemistry and source identification of
768 coarse and fine aerosols in an urban area of eastern central India. Atmos. Res. 95, 65-76.

769 Volkamer, R., Platt, U., Wirtz, K., 2001. Primary and secondary glyoxal formation from aromatics:
770 Experimental evidence for the bicycloalkyl-radical pathway from benzene, toluene, and p-
771 xylene. J. Phys. Chem. A 105, 7865-7874.

772 Wang, G.H., Kawamura, K., Cheng, C.L., Li, J.J., Cao, J.J., Zhang, R.J. et al., 2012. Molecular
773 distribution and stable carbon isotopic composition of dicarboxylic acids, ketocarboxylic
774 acids, and alpha-dicarbonyls in size-resolved atmospheric particles From Xi'an city, China.
775 Environ. Sci. Technol. 46, 4783-4791.

776 Wang, H., Kawamura, K., Shooter, D., 2005. Carbonaceous and ionic components in wintertime
777 atmospheric aerosols from two New Zealand cities: implications for solid fuel combustion.
778 Atmos. Environ. 39, 5865-5875.

779 Wang, Z., Bi, X., Sheng, G., Fu, J., 2009. Characterization of organic compounds and molecular
780 tracers from biomass burning smoke in south China 1: broad-leaf trees and shrubs. Atmos.
781 Environ. 43, 3096-3102.

782 Warneck P., 2003. In-cloud chemistry opens pathway to the formation of oxalic acid in the marine
783 atmosphere. Atmos. Environ. 37, 2423-2427.

784 Wu, S.-P., James, S., Liu, B.-L., Li, T.-C., Yuan, C.-S., 2015. Seasonal variations and source
785 identification of selected organic acids associated with PM_{10} in the coastal area of
786 Southestern China. Atmos. Res. 155, 37-51.

787 Yamasoe, M.A., Artaxo, P., Miguel, A.H., Allen, A.G., 2000. Chemical composition of aerosol
788 particles from direct emissions of vegetation fires in the Amazon Basin: water-soluble
789 species and trace elements. Atmos. Environ. 34, 1641-1653.

790 Zhao, J.P., Zhang, F.W., Xu, Y., Chen, J.S., 2011. Characterization of water-soluble inorganic ions
791 in size-segregated aerosols in coastal city, Xiamen. Atmos. Res. 99, 546-562.

792 Zhang, Y.L., Kawamura, K., Cao, F., Lee, M., 2016a. Stable carbon isotopic compositions of low-
793 molecular-weight dicarboxylic acids, oxocarboxylic acids, α-dicarbonyls, and fatty acids:
794 implications for atmospheric processing of organic aerosols. J. Geophys. Res. 121, 3707-
795 3717.

796 Zhang, Y.L., Kawamura, K., Fu, P.Q., Boreddy, S.K.R., Watanabe, T., Hatakeyama, S., Takami,
797 A., Wang, W., 2016b. Aircraft observations of water-soluble dicarboxylic acids in the
798 aerosols over China. Atmos. Chem. Phys. 16, 6407-6419.

799 Zhuang, H., Chan, C.K., Fang, M., Wexler, A.S., 1999. Formation of nitrate and non-sea-salt sulfate
800 on coarse particles. Atmos. Environ. 33, 4223-423.

801 Ziemann, P.J., 2005. Aerosol products, mechanisms, and kinetics of heterogeneous reactions with
802 oleic acid in pure and mixed particles. Faraday Discuss. 130, 469-490.

803 Zimmermann, J., Poppe, D., 1996. A supplement for the RADM2 chemical mechanism: the
804 photooxidation of isoprene. Atmos. Environ. 30, 1255-1269.

Tables:

Table 1
Concentrations of measured organic compounds and inorganic ions in fine and coarse mode aerosols in the urban atmosphere of central India in winter from December 2012 to February 2013.

Compounds	Abbreviation	Chemical formula	Fine mode				Coarse mode			
			Mean	S.D.[a]	Min.[b]	Max.[c]	Mean	S.D.	Min.	Max.
Dicarboxylic acids[d]										
Saturated normal-chain diacids										
Oxalic	C_2	HOOC-COOH	545	231	248	1041	367	117	231	628
Malonic	C_3	HOOC-CH_2-COOH	36.2	16.2	20.8	67.4	27.0	8.98	17.8	43.3
Succinic	C_4	HOOC-$(CH_2)_2$-COOH	113	30.3	77.4	175	82.5	26.0	51.6	134
Glutaric	C_5	HOOC-$(CH_2)_3$-COOH	23.0	6.76	15.1	36.1	17.4	6.99	8.81	33.9
Adipic	C_6	HOOC-$(CH_2)_4$-COOH	16.1	5.91	9.88	28.1	11.7	4.01	6.86	19.9
Pimelic	C_7	HOOC-$(CH_2)_5$-COOH	8.87	3.47	5.38	16.8	5.43	1.97	2.73	8.27
Suberic	C_8	HOOC-$(CH_2)_6$-COOH	10.2	8.36	0.00	28.5	5.48	5.32	0.00	14.5
Azelaic	C_9	HOOC-$(CH_2)_7$-COOH	81.3	29.8	38.2	155	79.9	24.5	52.2	132
Decanedioic	C_{10}	HOOC-$(CH_2)_8$-COOH	4.94	3.03	1.80	12.5	2.81	1.38	0.92	5.32
Undecanedioic	C_{11}	HOOC-$(CH_2)_9$-COOH	8.25	6.16	4.05	27.7	5.53	2.16	2.73	9.37
Dodecanedioic	C_{12}	HOOC-$(CH_2)_{10}$-COOH	0.45	0.46	0.00	1.59	0.11	0.31	0.00	1.11
Branched-chain diacids										
Methylmalonic	iC_4	HOOC-$CH(CH_3)$-COOH	2.20	0.80	0.97	3.93	2.42	0.74	1.01	4.07
Methylsuccinic	iC_5	HOOC-$CH(CH_3)$-COOH	21.5	6.16	12.5	33.0	21.6	5.92	13.0	31.6
2-Methylglutaric	iC_6	HOOC-$CH(CH_3)$-$(CH_2)_2$-COOH	2.10	0.64	1.15	3.21	2.32	0.85	1.26	4.34
Unsaturated aliphatic diacids										
Maleic	M	HOOC-CH=CH-COOH - *cis*	25.7	4.47	15.8	33.3	34.4	5.25	23.5	41.9
Fumaric	F	HOOC-CH=CH-COOH - *trans*	7.13	0.42	6.53	7.74	8.64	0.41	7.75	9.11
Methylmaleic	mM	HOOC-$C(CH_3)$=CH-COOH - *cis*	9.58	3.35	4.71	14.8	10.4	2.47	7.49	14.6
Unsaturated aromatic diacids										
Phthalic	Ph	HOOC-(C_6H_4)-COOH - *o*-isomer	64.6	28.5	22.0	140	70.7	25.8	22.0	129
Isophthalic	iPh	HOOC-(C_6H_4)-COOH - *m*-isomer	4.44	1.08	2.81	6.35	4.07	1.65	2.10	7.35
Terephthalic	tPh	HOOC-(C_6H_4)-COOH - *p*-isomer	74.8	58.4	19.5	185	31.9	23.2	10.4	79.4
Multifunctional diacids										
Malic	hC_4	HOOC-CH(OH)-CH_2-COOH	1.45	0.79	0.78	3.82	2.07	1.26	0.41	5.11
Ketomalonic	kC_3	HOOC-HC(O)-COOH	6.54	3.44	2.62	14.3	5.01	2.66	2.22	11.0
4-Ketopimelic	kC_7	HOOC-CH_2-CH_2-HC(O)$(CH_2)_2$-COOH	5.17	2.97	1.15	9.97	1.62	0.81	0.63	2.95
Total diacids			1072	375	678	1808	800	210	523	1204
ω-Oxocarboxylic acids[d]										
Glyoxylic	ωC_2	OHC-COOH	31.6	16.4	13.7	64.2	20.4	8.86	11.6	45.1
3-Oxopropanoic	ωC_3	OHC-CH_2-COOH	5.27	2.62	2.30	10.8	3.30	1.65	1.00	7.47
4-Oxobutanoic	ωC_4	OHC-$(CH_2)_2$-COOH	18.8	11.1	4.97	50.4	13.9	11.3	3.76	46.3
5-Oxopentanoic	ωC_5	OHC-$(CH_2)_3$-COOH	3.67	1.44	2.09	5.88	2.74	1.20	1.43	4.53
7-Oxoheptanoic	ωC_7	OHC-$(CH_2)_5$-COOH	7.57	3.95	2.66	14.9	1.95	0.73	1.06	3.14
8-Oxooctanoic	ωC_8	OHC-$(CH_2)_6$-COOH	9.13	5.28	2.84	17.0	1.79	0.63	0.78	2.67
9-Oxononanoic	ωC_9	OHC-$(CH_2)_7$-COOH	1.74	0.78	0.96	3.14	1.43	0.64	0.73	3.12
Total ω-oxoacids			77.8	36.9	40.8	160	45.5	22.2	22.8	111
Ketoacid[d]										
Pyruvic	Pyr	CH_3- C(O)-COOH	13.1	5.26	6.56	24.1	9.78	3.82	5.54	18.5
α-Dicarbonyls[d]										
Glyoxal	Gly	OHC-CHO	18.5	5.97	10.2	30.8	12.5	3.79	7.19	19.4
Methylglyoxal	MeGly	CH_3-C(O)-CHO	11.7	3.71	6.31	18.6	8.90	2.71	2.86	14.0
Total α-dicarbonyls			30.2	8.81	19.4	46.4	21.4	5.44	12.6	31.1
Anhydrosugar[e]										
Levoglucosan	Levo		2.18	0.83	1.09	3.62	0.61	0.22	0.29	1.02
Carbonaceous species[e]										
WSOC			15.3	4.79	8.78	25.8	8.39	2.05	4.08	11.5
OC			22.3	7.32	12.5	39.5	15.1	4.29	8.69	23.6
EC			3.73	3.01	1.15	11.9	1.18	0.92	0.35	3.67
TC			26.0	9.95	14.9	51.3	16.2	4.96	9.68	27.3
Ionic species[e]										
Na^+			1.38	0.43	0.67	1.96	1.95	0.76	0.87	3.39
NH_4^+			7.39	2.37	5.18	13.3	4.60	1.63	2.45	8.48
K^+			6.92	1.91	5.15	11.7	3.71	1.39	1.96	7.20
Mg^{2+}			0.65	0.33	0.26	1.22	1.68	0.56	0.93	3.00
Ca^{2+}			1.46	0.47	0.85	2.30	11.3	2.56	8.30	17.7
MSA^-			1.87	0.72	0.96	3.17	0.65	0.17	0.41	1.02
Cl^-			6.50	2.68	2.47	12.0	4.50	1.66	3.68	6.13
NO_3^-			8.36	3.47	3.02	13.7	6.78	0.77	5.59	7.90
SO_4^{2-}			15.9	3.52	10.5	23.2	7.79	1.90	5.25	12.9
Total water-soluble ions			50.4	13.6	32.1	79.2	42.9	8.98	34.1	67.8

Fine mode represents aerosol size of D_p < 2.1 µm. Coarse mode represents aerosol size of D_p > 2.1 µm. [a]Standard deviation. [b]Minimum. [c]Maximum. [d]Values are in ng m^{-3}. [e]Values are in µg m^{-3}.

Table 2
Pearson correlation analysis among measured ionic species and organic compounds in fine[a] and coarse[b] mode aerosols in the urban atmosphere of central India in winter from December 2012 to February 2013.

	Na^+	NH_4^+	K^+	Mg^{2+}	Ca^{2+}	Cl^-	NO_3^-	SO_4^{2-}	MSA^-	WSOC	OC	EC	C_2	C_3	C_4	C_5	C_9	ωC_2	ωC_3	ωC_4	ωC_5	ωC_9	Gly	MeGly	Levo
Na^+		0.55	0.55	0.57	0.67	0.55	0.21	0.13	0.22	0.47	0.38	0.53	0.63	0.40	0.43	0.58	0.40	0.65	0.60	0.41	0.55	0.22	0.31	0.21	0.53
NH_4^+	0.68		0.98	0.12	0.10	0.78	0.67	0.85	0.83	0.72	0.79	0.80	0.83	0.83	0.81	0.86	0.93	0.80	0.90	0.92	0.86	0.63	0.76	0.58	0.96
K^+	0.69	0.96		0.18	0.22	0.78	0.57	0.85	0.83	0.73	0.80	0.88	0.83	0.82	0.81	0.87	0.93	0.81	0.90	0.92	0.87	0.68	0.86	0.59	0.98
Mg^{2+}	0.66	0.98	0.98		0.91	0.23	0.51	0.03	0.01	0.51	0.03	0.05	0.36	0.05	0.23	0.07	0.12	0.12	0.52	0.21	0.25	0.18	0.55	0.21	0.09
Ca^{2+}	0.70	0.93	0.93	0.97		0.35	0.41	0.35	0.36	0.36	0.40	0.48	0.30	0.48	0.13	0.16	0.28	0.11	0.52	0.33	0.27	0.12	0.39	0.11	0.08
Cl^-	0.22	0.56	0.59	0.66	0.73		0.53	0.90	0.81	0.52	0.69	0.66	0.53	0.52	0.66	0.61	0.83	0.48	0.63	0.80	0.62	0.11	0.73	0.48	0.88
NO_3^-	0.17	0.41	0.42	0.56	0.68	0.72		0.53	0.56	0.52	0.59	0.36	0.43	0.50	0.53	0.57	0.57	0.43	0.69	0.49	0.59	0.08	0.35	0.21	0.58
SO_4^{2-}	0.13	0.66	0.69	0.63	0.65	0.73	0.42		0.91	0.56	0.62	0.60	0.65	0.43	0.69	0.62	0.83	0.50	0.62	0.68	0.67	0.55	0.40	0.81	0.85
MSA^-	0.50	0.97	0.96	0.36	0.32	0.51	0.38	0.73		0.42	0.55	0.55	0.57	0.55	0.66	0.70	0.79	0.53	0.66	0.72	0.79	0.16	0.56	0.77	0.89
WSOC	0.17	0.52	0.53	0.48	0.65	0.41	0.62	0.57	0.53		0.96	0.78	0.92	0.73	0.92	0.83	0.72	0.80	0.85	0.70	0.63	0.61	0.52	0.46	0.92
OC	0.41	0.66	0.67	0.58	0.63	0.42	0.52	0.65	0.65	0.90		0.82	0.89	0.80	0.91	0.85	0.83	0.82	0.89	0.78	0.70	0.59	0.52	0.52	0.85
EC	0.69	0.90	0.92	0.55	0.61	0.50	0.18	0.60	0.86	0.46	0.69		0.85	0.73	0.78	0.85	0.82	0.83	0.88	0.87	0.78	0.33	0.66	0.65	0.88
C_2	0.28	0.61	0.63	0.59	0.63	0.60	0.69	0.62	0.60	0.83	0.82	0.66		0.80	0.90	0.92	0.80	0.91	0.90	0.72	0.80	0.61	0.65	0.63	0.95
C_3	0.38	0.57	0.57	0.46	0.56	0.07	0.60	0.42	0.58	0.77	0.83	0.63	0.70		0.80	0.86	0.81	0.90	0.83	0.56	0.87	0.69	0.76	0.45	0.83
C_4	0.18	0.69	0.69	0.63	0.58	0.55	0.62	0.83	0.75	0.65	0.72	0.78	0.81	0.69		0.93	0.80	0.75	0.85	0.82	0.73	0.51	0.61	0.70	0.92
C_5	0.30	0.73	0.73	0.68	0.55	0.26	0.63	0.60	0.81	0.53	0.62	0.79	0.63	0.73	0.88		0.80	0.87	0.93	0.78	0.90	0.53	0.72	0.65	0.86
C_9	0.15	0.67	0.65	0.63	0.65	0.29	0.66	0.48	0.72	0.55	0.57	0.55	0.37	0.57	0.61	0.71		0.79	0.87	0.83	0.79	0.62	0.55	0.69	0.98
ωC_2	0.56	0.87	0.89	0.83	0.79	0.61	0.22	0.80	0.85	0.57	0.69	0.95	0.76	0.63	0.82	0.80	0.53		0.88	0.69	0.87	0.56	0.85	0.53	0.90
ωC_3	0.43	0.81	0.83	0.79	0.75	0.59	0.21	0.79	0.81	0.77	0.80	0.85	0.90	0.71	0.85	0.81	0.57	0.93		0.80	0.88	0.45	0.67	0.57	0.82
ωC_4	0.32	0.63	0.67	0.69	0.72	0.83	0.42	0.80	0.60	0.59	0.58	0.67	0.81	0.29	0.63	0.43	0.29	0.78	0.83		0.72	0.07	0.46	0.73	0.90
ωC_5	0.20	0.77	0.76	0.80	0.71	0.55	0.35	0.60	0.81	0.50	0.43	0.58	0.45	0.33	0.53	0.60	0.80	0.63	0.67	0.60		0.38	0.83	0.67	0.89
ωC_9	0.06	0.10	0.08	0.56	0.61	0.23	0.60	0.22	0.12	0.55	0.56	0.02	0.48	0.36	0.32	0.06	0.60	0.07	0.23	0.20	0.21		0.42	0.13	0.80
Gly	0.25	0.70	0.68	0.60	0.63	0.22	0.59	0.59	0.76	0.48	0.65	0.72	0.48	0.69	0.78	0.82	0.87	0.63	0.63	0.31	0.61	0.12		0.63	0.92
MeGly	0.23	0.32	0.32	0.35	0.59	0.38	0.55	0.48	0.41	0.26	0.12	0.32	0.53	0.20	0.63	0.60	0.33	0.43	0.53	0.47	0.49	0.36	0.38		0.60
Levo	0.08	0.38	0.50	0.05	0.02	0.15	0.21	0.39	0.09	0.50	0.62	0.80	0.60	0.52	0.63	0.66	0.63	0.62	0.60	0.58	0.63	0.68	0.55	0.28	

See Table 1 for abbreviation. [a]See upper diagonal triangle. [b]See lower diagonal triangle. $P \leq 0.01$ for the correlation where r is ≥ 0.69. $P \leq 0.05$ for the correlation where r is 0.56 to 0.68.

807

Figure captions:

Fig. 1. A map showing the geographical location of Raipur (21.2°N and 82.3°E) in India with its surroundings in Asia.

Fig. 2. NOAA HYSPLIT seven-day backward air mass trajectories at 500 m above ground level for the observation site in winter of 2012-2013.

Fig. 3. Average chemical composition (%) of size-segregated aerosols collected in the urban atmosphere of Raipur in central India during the study period. We defined cutoff size of 2.1 μm as a split diameter between the fine and coarse mode aerosol. The abundance of organic matter (OM) was calculated by multiplying the concentrations of OC with the conversion factor of 1.6 as suggested for urban aerosols by Turpin and Lim (2001).

Fig. 4. Average molecular distributions of water-soluble dicarboxylic acids and related polar compounds in size-segregated aerosols.

Fig. 5. Average size distribution of concentrations of measured water-soluble major ions in aerosol particles collected in central India. The error bars represent one standard deviation.

Fig. 6. Average size distribution of concentrations of water-soluble organic carbon (WSOC), organic carbon (OC), elemental carbon (EC) and levoglucosan in aerosol particles collected in central India. The error bars represent one standard deviation.

Fig. 7. Average size distribution of concentrations of measured dicarboxylic acids in aerosol particles collected in central India. The error bars represent one standard deviation.

Fig. 8. Box-and-whisker diagrams of ratios of diacids in size-segregated aerosols. Lower and upper ends of the box show the quartiles at 25% and 75% whereas upper and lower bars of the whiskers present the quartiles at 10% and 90%. The cross bar in the box shows the median and round circle shows the average value.

Fig. 9. Average size distribution of concentrations of measured ω-oxocarboxylic acids and pyruvic acid in aerosol particles collected in central India. The error bars represent one standard deviation.

Fig. 10. Average size distribution of concentrations of measured α-dicarbonyls in aerosol particles collected in central India. The error bars represent one standard deviation.

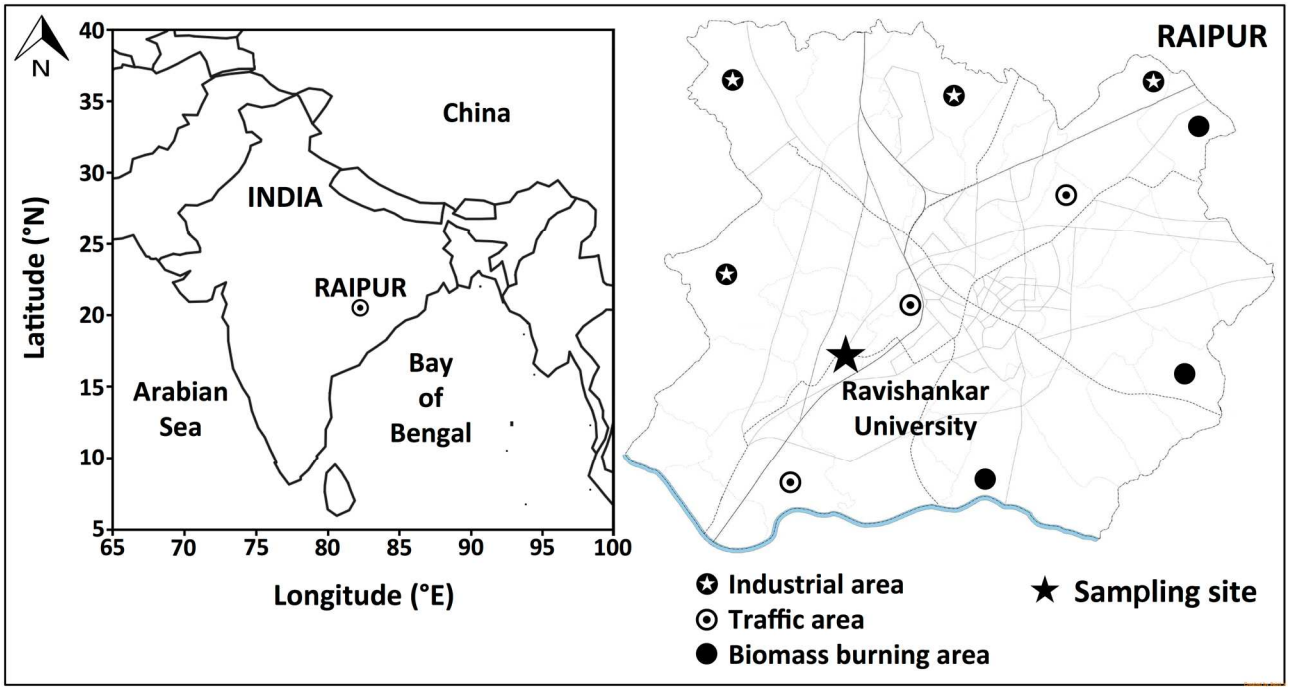

835

836 **Fig. 1.** A map showing the geographical location of Raipur (21.2°N and 82.3°E) in India with its

837 surroundings in Asia.

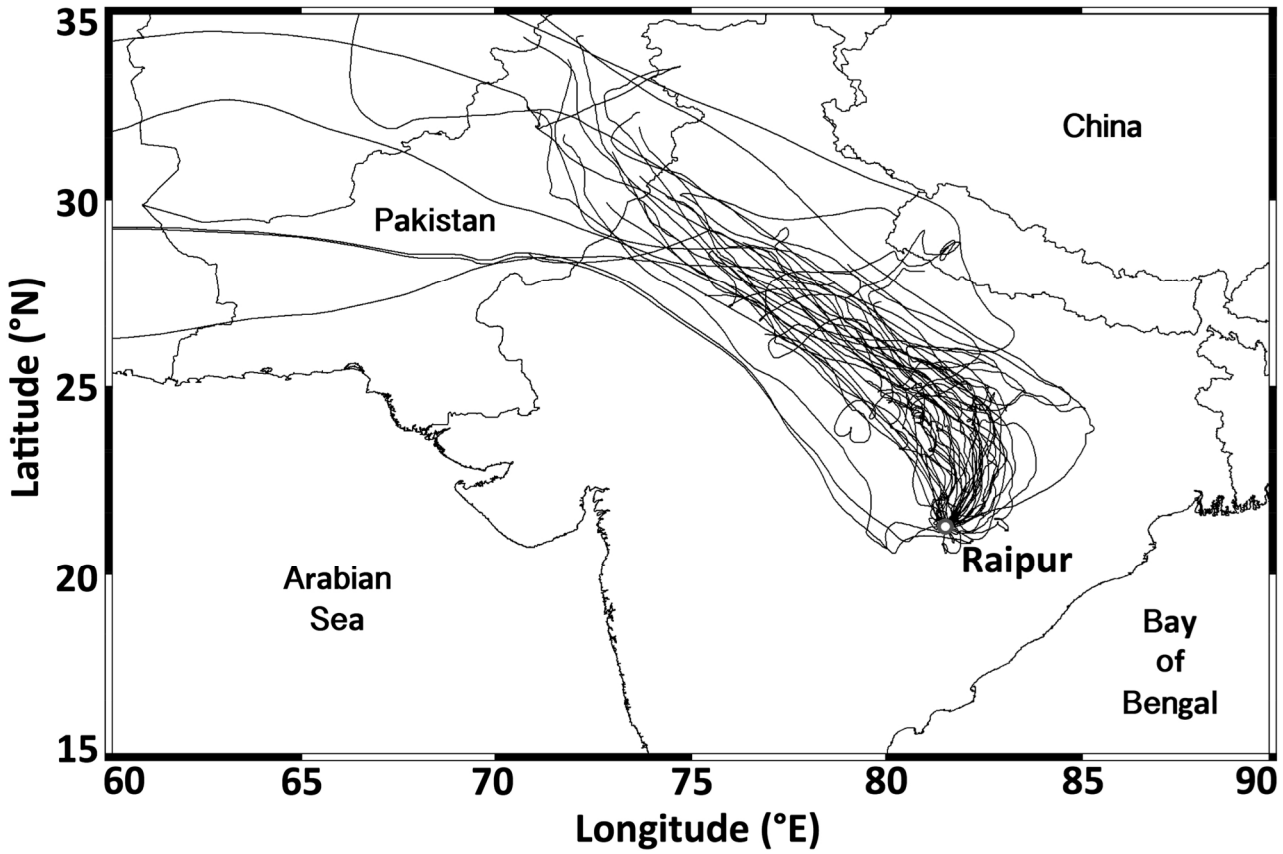

838

839 **Fig. 2.** NOAA HYSPLIT seven-day backward air mass trajectories at 500 m above ground level for

840 the observation site in winter of 2012-2013.

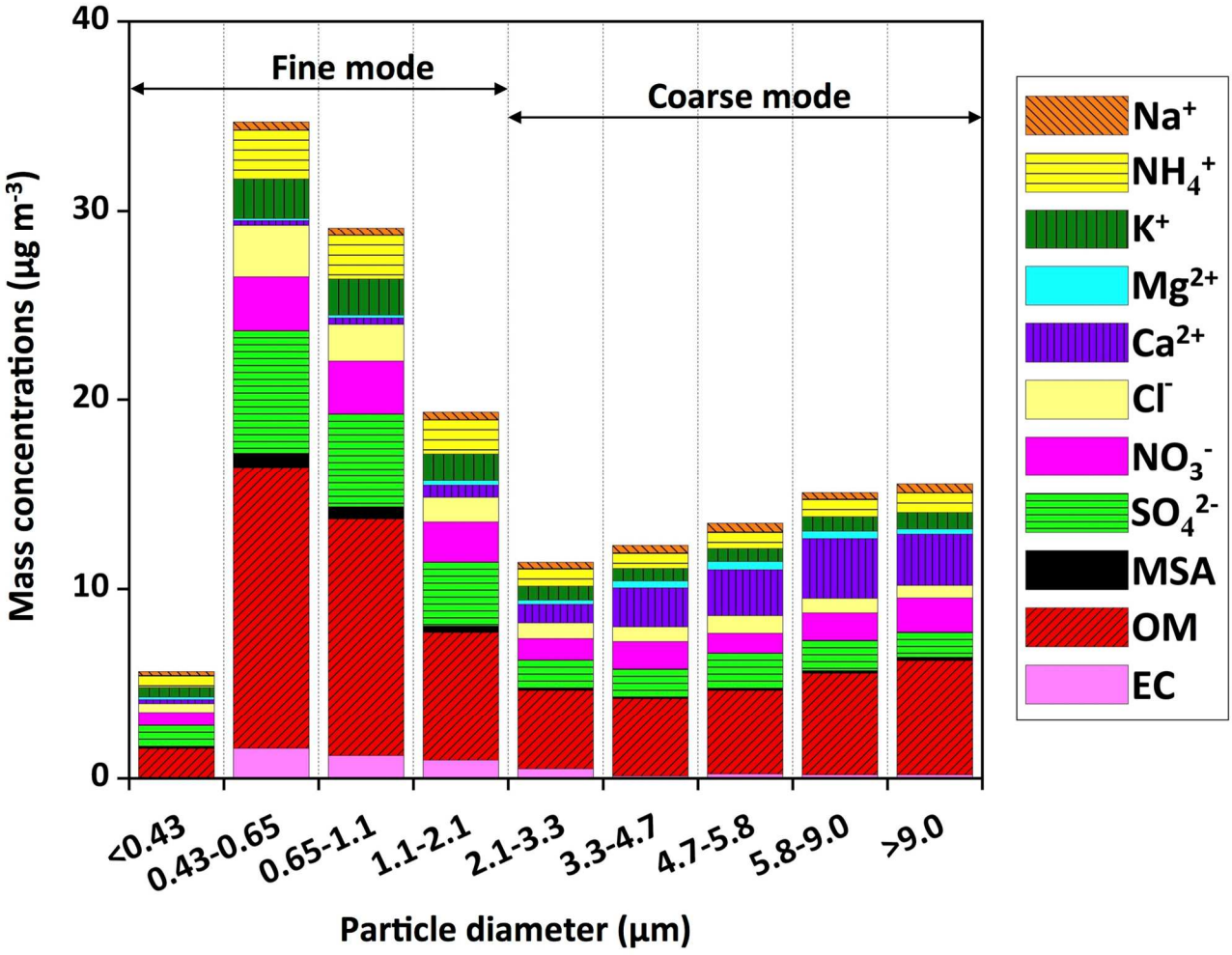

841

842 **Fig. 3.** Average chemical composition of size-segregated aerosols collected in the urban atmosphere
843 of Raipur in central India during the study period. We defined cutoff size of 2.1 µm as a split
844 diameter between the fine and coarse mode aerosol. The abundance of organic matter (OM) was
845 calculated by multiplying the concentrations of OC with the conversion factor of 1.6 as suggested
846 for urban aerosols by Turpin and Lim (2001).

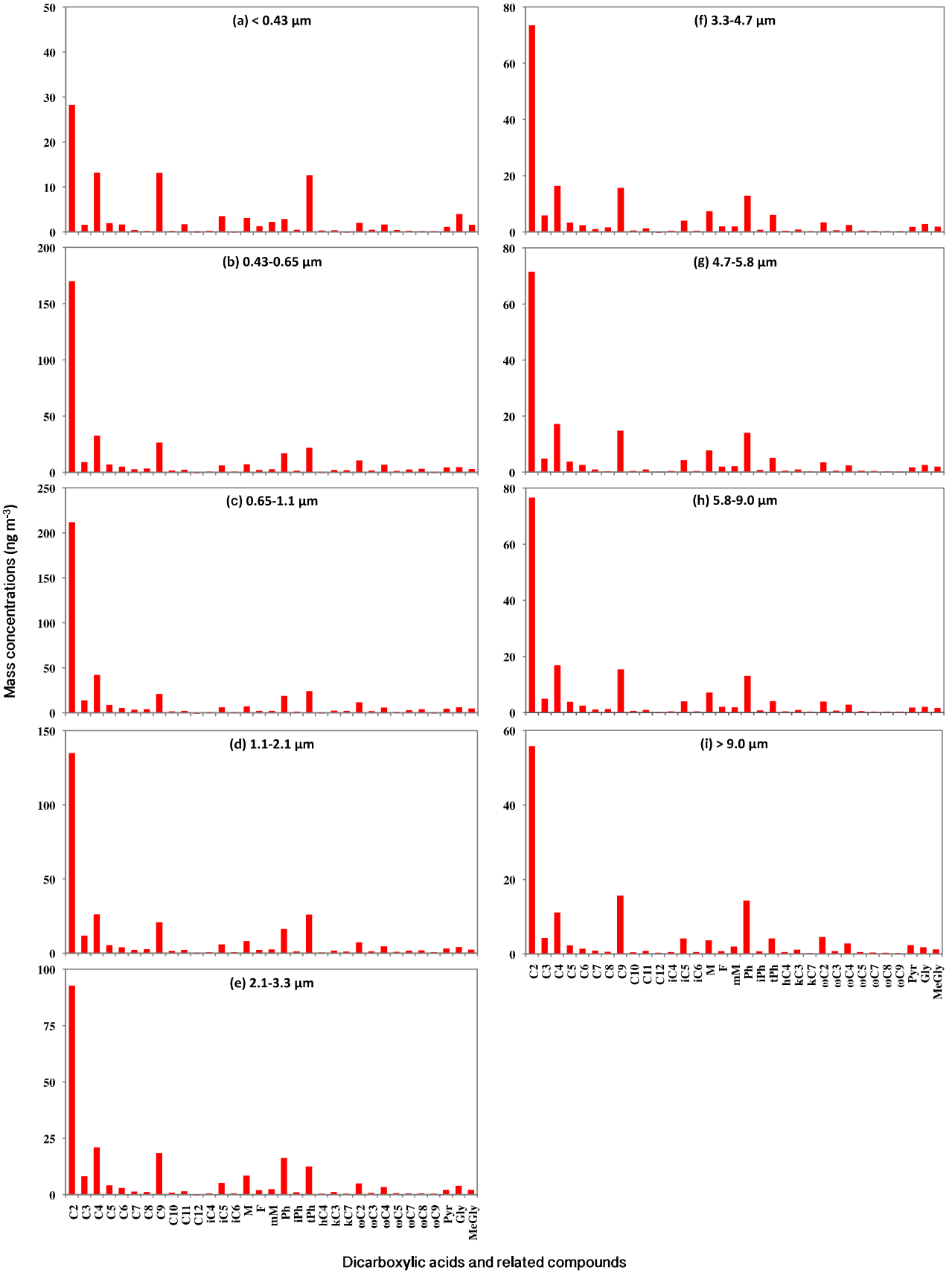

847

848 **Fig. 4.** Average molecular distributions of water-soluble dicarboxylic acids and related polar

849 compounds in size-segregated aerosols.

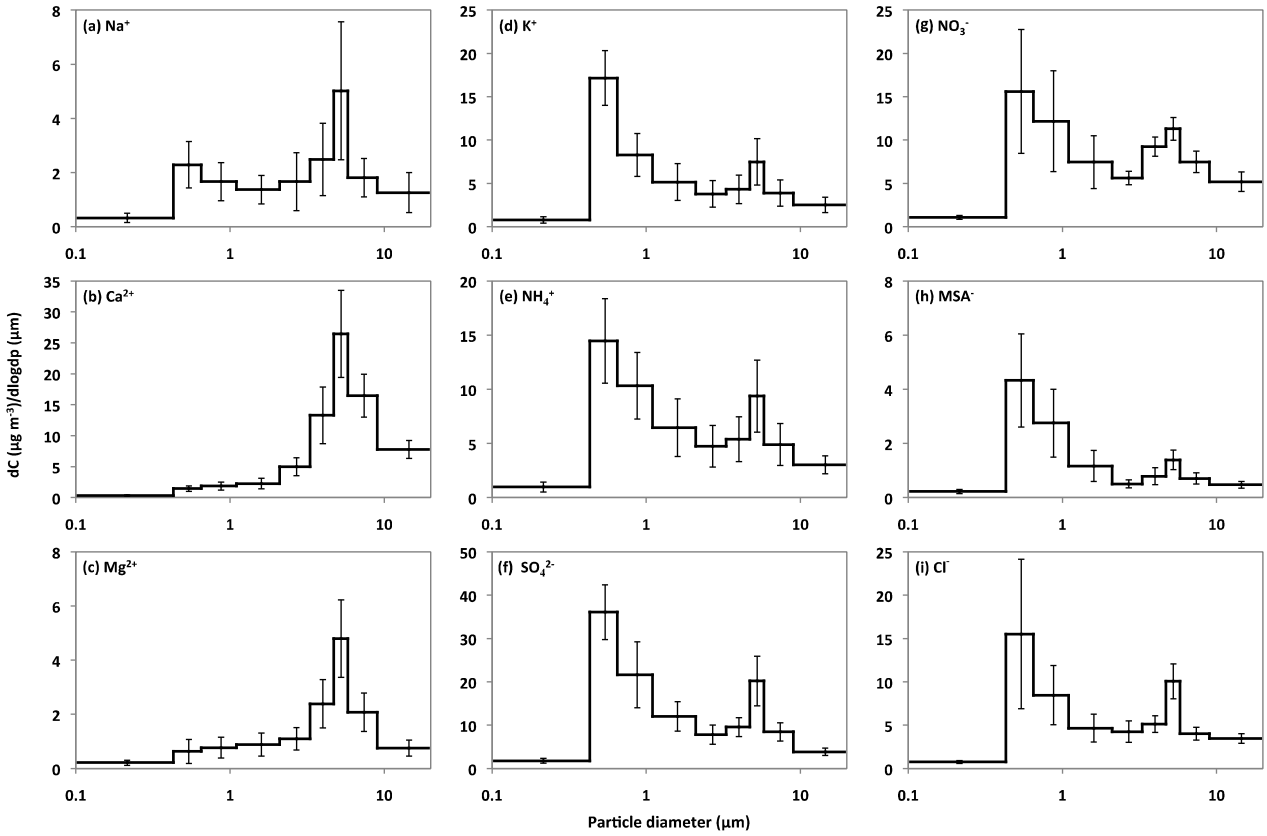

850

851 **Fig. 5.** Average size distribution of concentrations of measured water-soluble major ions in aerosol

852 particles collected in central India. The error bars represent one standard deviation.

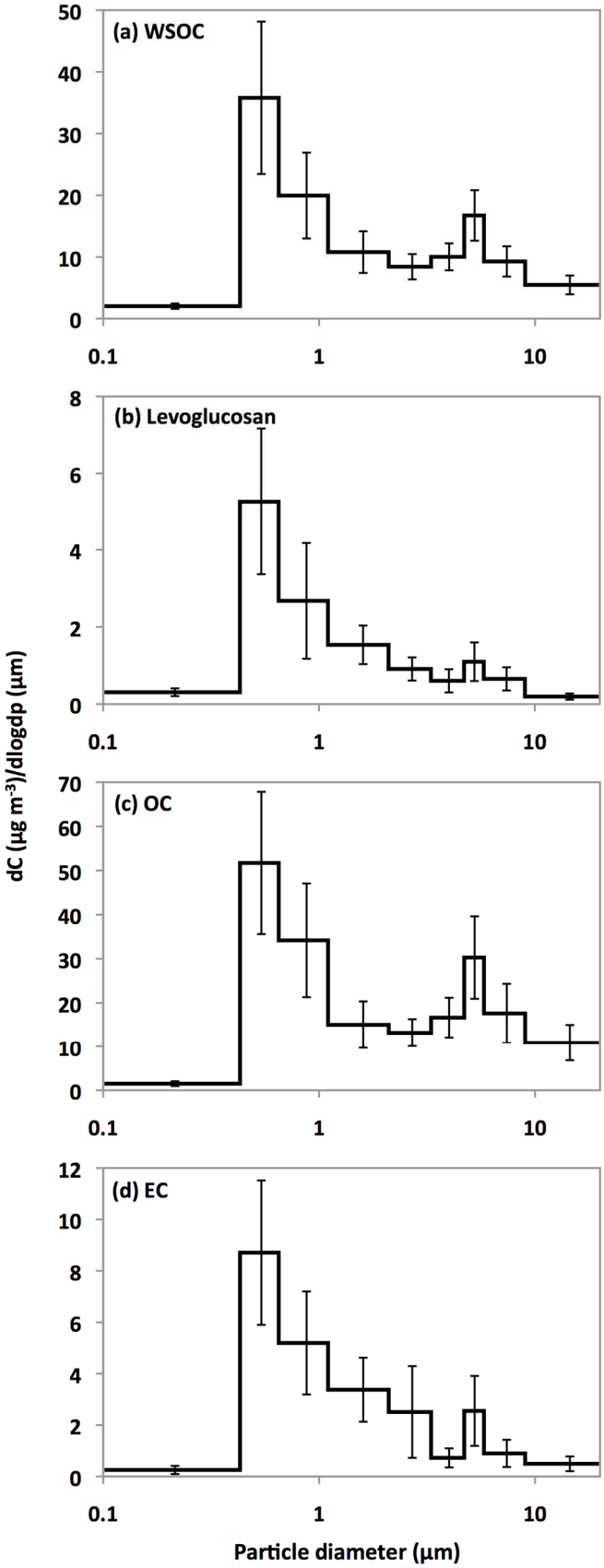

853

854 **Fig. 6.** Average size distribution of concentrations of water-soluble organic carbon (WSOC),
855 organic carbon (OC), elemental carbon (EC) and levoglucosan in aerosol particles collected in
856 central India. The error bars represent one standard deviation.

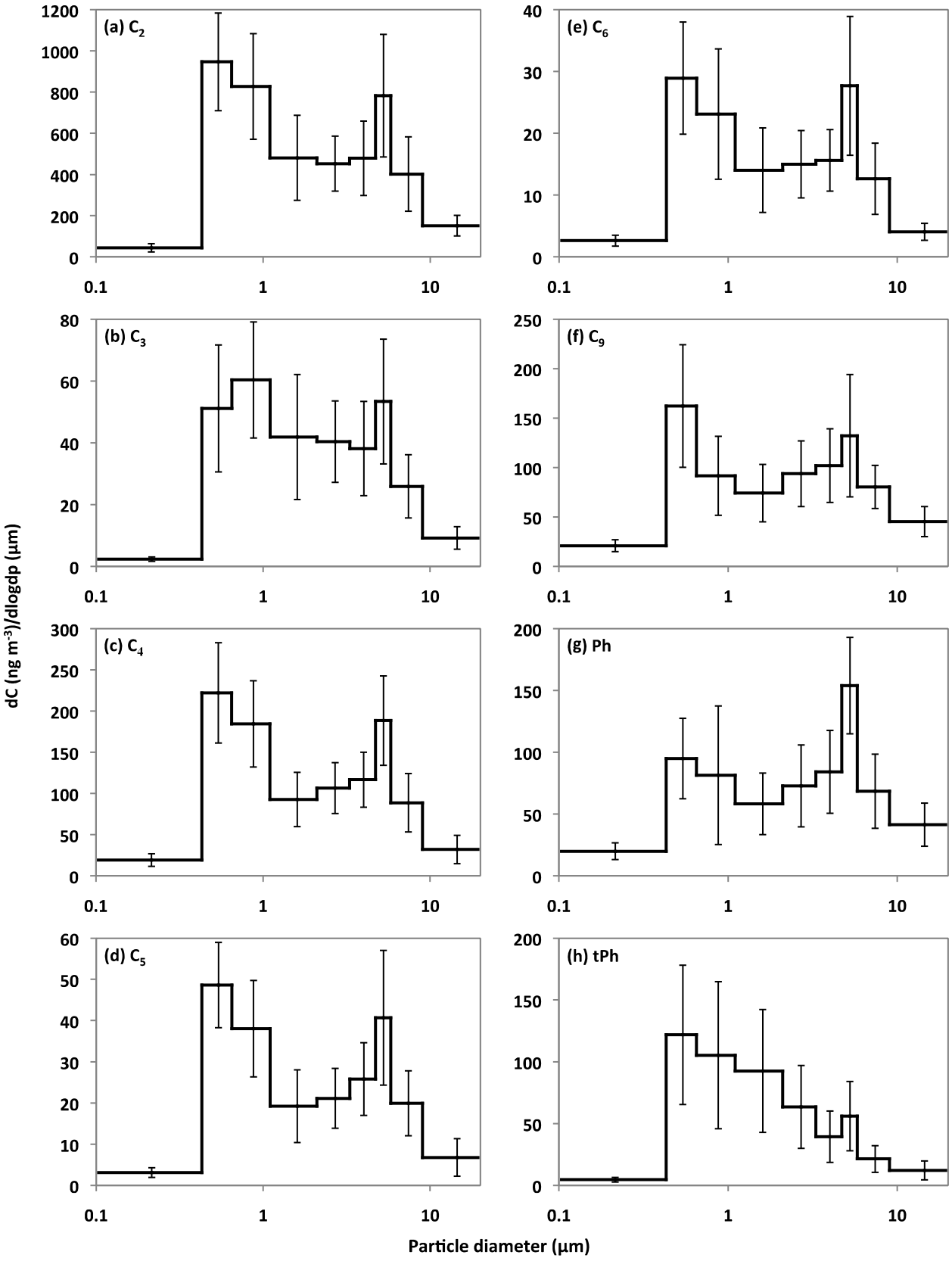

857

858 **Fig. 7.** Average size distribution of concentrations of measured dicarboxylic acids in aerosol

859 particles collected in central India. The error bars represent one standard deviation.

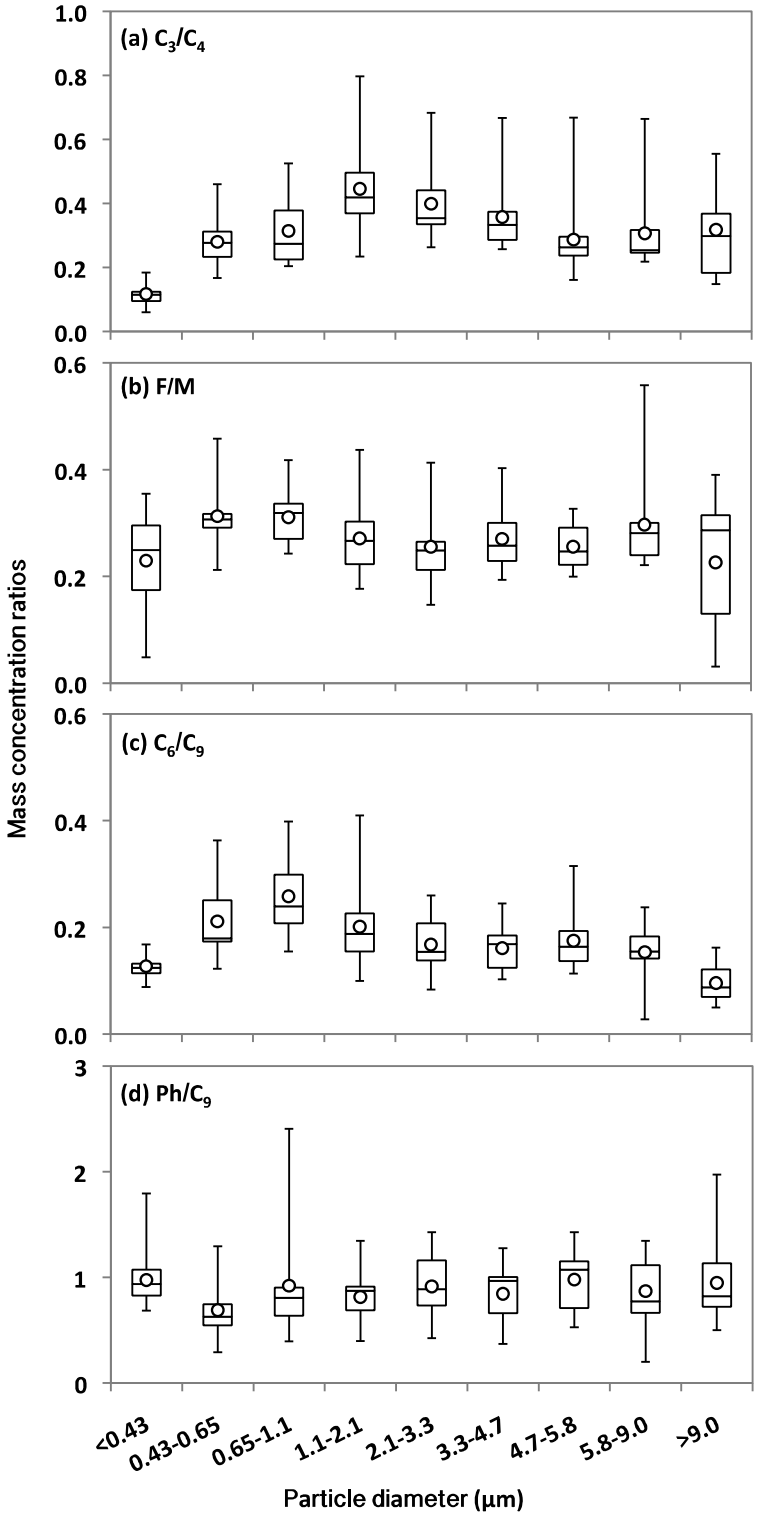

860

861 **Fig. 8.** Box-and-whisker diagrams of ratios of diacids in size-segregated aerosols. Lower and upper
862 end of the box show the quartiles at 25% and 75% whereas upper and lower bars of the whiskers
863 present the quartiles at 10% and 90%. The cross bar in the box shows the median and round circle
864 shows the average value.

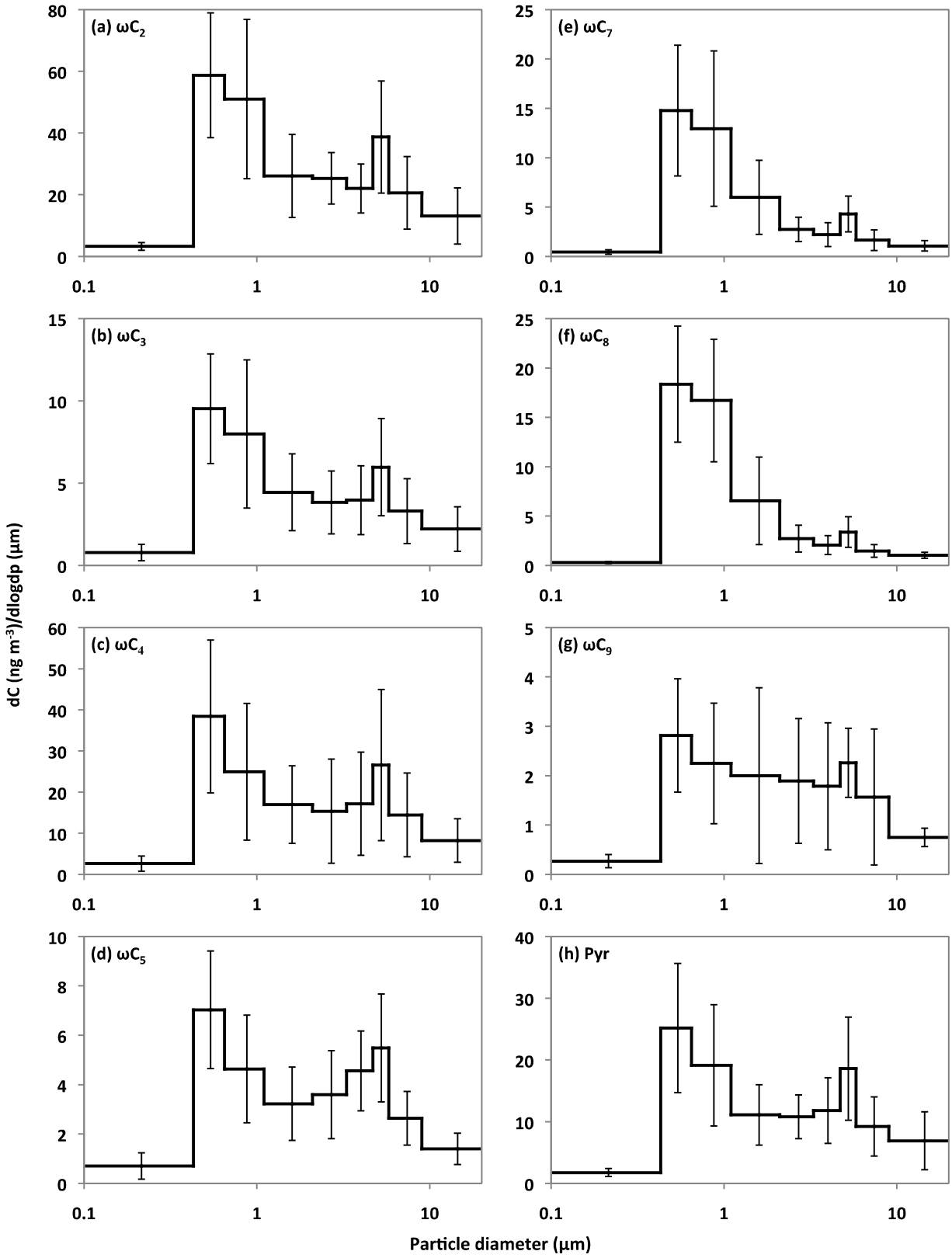

865

866 **Fig. 9.** Average size distribution of concentrations of measured ω-oxocarboxylic acids and pyruvic

867 acid in aerosol particles collected in central India. The error bars represent one standard deviation.

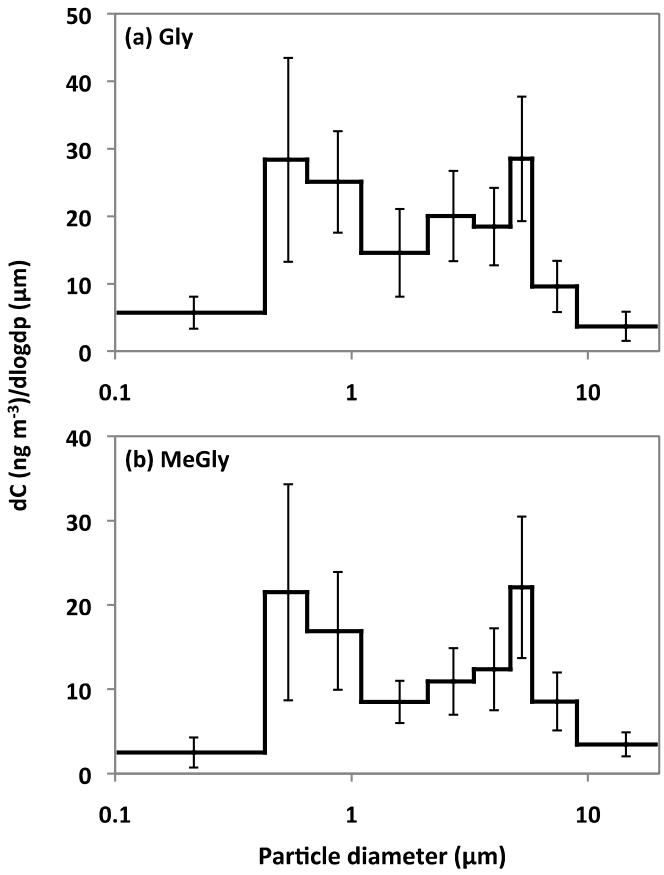

868

869 **Fig. 10.** Average size distribution of concentrations of measured α-dicarbonyls in aerosol particles

870 collected in central India. The error bars represent one standard deviation.